Mathematical Modeling of Molecular Weight Distributions in Vinyl Chloride Suspension Polymerizations Performed with a Bifunctional Initiator through Probability Generating Functions

Carlos A. Castor Jr., Claudia Sarmoria, Mariano Asteasuain, Adriana Brandolin, José C. Pinto*

This paper presents a mathematical model to describe the evolution of the molecular weight distribution (MWD) in vinyl chloride (VCM) free-radical suspension polymerizations performed with a bifunctional initiator, 1,3-di(2-neodecanoylperoxyisopropyl) (DIPND). The model yields, as a function of time, the mass balances for the distinct phases, the monomer conversion, the number- and mass-average molecular weights and the complete MWD of both the growing and dead polymer chains. In order to describe the MWD, the model uses probability generating functions (pgf) to transform the mass balance equations into a reduced and finite set of model equations. As shown throughout many examples, the MWD's of the final polymer resin is little sensitive to the presence of the linear symmetrical bifunctional initiator.

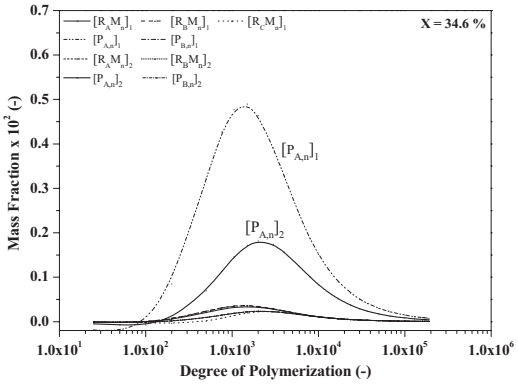

1. Introduction

Polymer materials are usually composed of chains of different sizes and compositions. The distributions of chain sizes and compositions are directly related to various physical properties, such as the elastic and loss moduli, melt viscosity, and crystallinity, among others.[1] Understanding the phenomena that affect those distributions can help in controlling the final properties of a particular polymer.

Poly(vinyl chloride) (PVC) is considered to be the most versatile of the commodity polymeric materials. This is mainly due to its low price, excellent processability and interesting properties, such as chemical inertness, low flammability, and flame retardancy. PVC is also compatible with many additives, including plasticizers, heat stabilizers, lubricants, and fillers. Commercially, PVC resins are obtained via bulk, solution, emulsion, and suspension polymerizations. With a worldwide production share of approximately 80%, suspension polymerization is the commonest PVC production process.[2]

Dr. C. Sarmoria, Dr. M. Asteasuain, Dr. A. Brandolin
Planta Piloto de Ingeniería Química – UNS-CONICET, Camino La Carrindanga, km 7 8000, Bahía Blanca, Argentina
Dr. C. A. Castor Jr., Dr. J. C. Pinto
Programa de Engenharia Química/COPPE, Universidade Federal do Rio de Janeiro, Cidade Universitária, CP 68502, Rio de Janeiro 21941-972, RJ, Brazil
E-mail: pinto@peq.coppe.ufrj.br,
Tel: +55-21-25628337, Fax: +55-21-25628300

DOI: 10.1002/mats.201400038

Since the second half of the 1980 s, several experimental studies and mathematical models regarding the use of multifunctional free radical initiators have been reported, mostly related to the production of poly(styrene) (PS),[3–9] poly(methyl methacrylate) (PMMA),[10,11] poly(vinyl acetate) (PVAc),[12] and styrene/methacrylate copolymers.[13] In most cases, polymerizations have been performed in bulk or solution processes. The use of multifunctional initiators is a mean to control the shape of the molecular weight distribution (MWD) and also to increase the average molecular weight averages, when reactions must be performed at high temperatures without significant modification of the production technology.

Regarding the specific case of vinyl chloride free radical polymerization, several mathematical models were developed to describe the kinetics of bulk and suspension polymerizations in the last 50 years.[14–21] Monofunctional initiators were used almost always. As the use of multifunctional initiators for production of PVC is still incipient, the related open literature is extremely scarce. To the best of our knowledge, a single study was reported in this field,[22] where the authors mixed bifunctional (1,3-di(2-neodecanoylperoxyisopropyl)benzene) (DIPND) and monofunctional initiators in order to evaluate the impact on the process operation. The authors presented experimental results collected from an industrial process and developed a model to represent the process behavior, calculating, among other parameters, the rate of polymerization and the number- and weight-average molecular weights, but not the full MWD. The authors also compared the efficiencies of bifunctional and monofunctional initiators, showing that bifunctional initiators allowed for reduction of the reaction time and implementation of smoother polymerization rate profiles. As experiments were not performed at similar operation conditions (for instance, similar active oxygen concentrations) and MWDs were not presented, it was not possible to evaluate the impact of the bifunctional initiator on the final properties of the obtained polymer material.

The main factor that has prevented the widespread use of bifunctional initiators in vinyl chloride polymerization processes is the low rate of thermal decomposition of most commercially available initiators at the feasible PVC process temperatures (40–60 °C). The vast majority of commercial multifunctional peroxides are used at reaction temperatures above 90 °C.[3–12] The lack of further studies regarding the use of multifunctional initiators in vinyl chloride free radical polymerizations is very intriguing, since the available results[22] highlighted the potential benefits of using multifunctional initiators in PVC processes.

As it is well known, average properties, such as the number- and weight-average molecular weights, are not sufficient to fully describe the properties of a polymer material. When one needs to predict rheological or flow properties, the full MWD becomes essential. On a more fundamental level, the association of measured MWD's with simulation results obtained for a particular process can provide insights into the kinetics of the polymerization process.

Several mathematical models and numerical approaches have been proposed to deal with the calculation of MWD's in polymerization processes,[8,23–37] including Monte Carlo procedures,[30] orthogonal collocation on finite elements,[31] discrete weighted Galerkin techniques,[32] sectional grid methods,[33] Laplace transforms,[27] and probability generating functions (pgf),[8] among others. Interestingly, few works have reported the calculation of MWDs for PVC.[34–36]

In the present study, a mathematical model is proposed to describe the vinyl chloride free radical suspension polymerization performed with bifunctional initiators in a batch reactor. The mathematical model is able to describe monomer conversions, mass compositions for each phase, number- and weight-average molecular weights and the complete MWD of both the growing and dead polymer chains as functions of time. In order to calculate the MWD, the pgf technique is used here. The pgf technique has been successfully implemented to describe MWD's in bulk styrene polymerizations, controlled polypropylene degradations, graft copolymerizations of polystyrene and polyethylene, among other reacting systems.[37,38] In order to validate the kinetic mechanism proposed in the present work, the experimental data presented by Krallis et al.[22] are used as references. The simulation results obtained here coincide with the published results when comparative analyses are possible, although the full MWD's are also presented here for different operating temperatures and initiator concentrations, as the consequence of the successful implementation of the pgf technique. To the best of our knowledge, this is the first study to describe theoretically the MWD of PVC synthesized by bifunctional initiators. Additionally, this is the first time that the pgf approach is used successfully to describe a multiphase reacting system in the presence of multiple growing macromolecular species, as described in the following sections.

2. Mathematical Model

2.1. Kinetics

The kinetic model proposed here is subject to the following hypotheses:

i) all kinetic constants are independent of the polymer chain length;

ii) the long chain approximation is valid;
iii) chain branching is neglected;
iv) non-polymeric radicals react with monomeric or polymeric radicals at the same rate;
v) stereochemical effects can be neglected;
vi) the reactor contains up to four phases: gaseous, aqueous, monomeric, and polymeric phases, which vary as the reaction proceeds;
vii) the reaction takes place in two phases (monomeric and polymeric);
viii) chain transfer to polymer and to initiator are negligible;
ix) primary radical termination is negligible;
x) there is no radical transfer between the monomeric and polymeric phases;
xi) homogeneity of the monomer droplets (the concentrations of initiator and radicals are the same in all of them);
xii) equal initiator concentration in the monomeric and polymeric phases;
xiii) constant efficiency of the initiators in monomeric and polymeric phases until the end of the second stage of polymerization;
xiv) the efficiency of the initiators in the third stage is controlled by diffusion, according to the free-volume theory.

It is assumed that polymerization reactions are performed in presence of the symmetrical bifunctional initiator DIPND. The decomposition reaction is shown in Figure 1.

The mechanism that leads to formation of diradicals has been the subject of some discussion. Since the initiation step is extremely fast and the resulting radicals are highly reactive, it is very difficult to ascertain experimentally whether diradicals are produced from primary monoradicals R_B or from macroradicals R_BM_n, $n=1, \ldots, \infty$. Some studies in the literature[22,39] consider that, after the first decomposition step shown in Figure 1, R_B may undergo

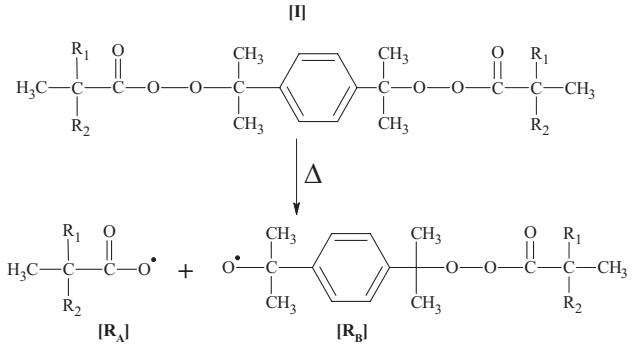

Figure 1. Schematic representation of the decomposition of bifunctional initiator DIPND.

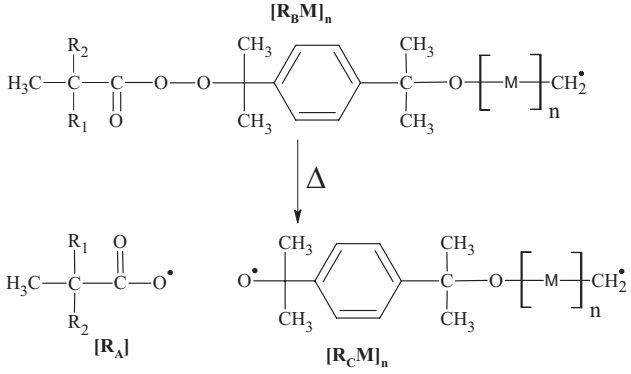

Figure 2. Structural representation of the decomposition of a polymer chain with an undecomposed peroxide.

decomposition to give a primary diradical. In this work, it is postulated that R_B can only take part of propagation reactions that lead to macroradicals R_BM_n, $n=1, \ldots \infty$, which are the ones that decompose to give macro-diradicals R_CM_n, as shown in Figure 2 and in accordance with Benbachir and Benjelloun.[4]

Although there are few literature reports on the formation of short branches in PVC chains through backbiting, such as ethyl (EB) and methyl (MB) branches, as well as chloroallylic end groups,[40,41] the proposed model does not consider these reaction steps at this point.

Assuming that the hypotheses stated above are valid, the following kinetic mechanism can be proposed for the free radical suspension polymerization of vinyl chloride:

Formation of primary radicals
Decomposition

$$I \xrightarrow{k_d} R_A + R_B \quad (1)$$

Initiation

$$R_A + M \xrightarrow{k_{iA}} R_A M_1 \quad (2)$$

$$R_B + M \xrightarrow{K_{iB}} R_B M_1 \quad (3)$$

Propagation

$$R_A M_n + M \xrightarrow{k_p} R_A M_{n+1} \quad (4)$$

$$R_B M_n + M \xrightarrow{k_p} R_B M_{n+1} \quad (5)$$

$$R_C M_n + M \xrightarrow{2k_p} R_C M_{n+1} \quad (6)$$

Chain transfer (to monomer)

$$R_A M_n + M \xrightarrow{k_{tr}} P_{A,n} + R_M \quad (7)$$

$$R_B M_n + M \xrightarrow{k_{tr}} P_B M_n + R_M \quad (8)$$

$$R_C M_n + M \xrightarrow{2k_{tr}} R_A M_n + R_M \quad (9)$$

Termination reactions
By combination

$$R_A M_n + R_A M_m \xrightarrow{k_{tc}} P_{A,m+n} \quad (10)$$

$$R_A M_n + R_B M_m \xrightarrow{k_{tc}} P_B M_{m+n} \quad (11)$$

$$R_A M_n + R_C M_m \xrightarrow{2k_{tc}} R_A M_{m+n} \quad (12)$$

$$R_B M_n + R_B M_m \xrightarrow{k_{tc}} P_{2B} M_{m+n} \quad (13)$$

$$R_B M_n + R_C M_m \xrightarrow{2k_{tc}} R_B M_{m+n} \quad (14)$$

$$R_C M_n + R_C M_m \xrightarrow{4k_{tc}} R_C M_{m+n} \quad (15)$$

By disproportionation

$$R_A M_n + R_A M_m \xrightarrow{k_{td}} P_{A,n} + P_{A,m} \quad (16)$$

$$R_A M_n + R_B M_m \xrightarrow{k_{td}} P_{A,n} + P_B M_m \quad (17)$$

$$R_A M_n + R_C M_m \xrightarrow{2k_{td}} P_{A,n} + R_A M_m \quad (18)$$

$$R_B M_n + R_B M_m \xrightarrow{k_{td}} P_B M_n + P_B M_m \quad (19)$$

$$R_B M_n + R_C M_m \xrightarrow{k_{td}} P_B M_n + R_A M_m \quad (20)$$

$$R_C M_n + R_C M_m \xrightarrow{4k_{td}} R_A M_n + R_A M_m \quad (21)$$

Reinitiation of live and dead polymer chains

$$R_B M_n \xrightarrow{k_{dr}} R_C M_n + R_A \quad (22)$$

$$P_B M_n \xrightarrow{k_{dp}} R_A M_n + R_A \quad (23)$$

$$P_{2B} M_n \xrightarrow{2k_{dp}} R_B M_n + R_A \quad (24)$$

Inhibition of live radical chains

$$R_A M_n + Z \xrightarrow{k_z} P_{A,n} + Z\bullet \quad (25)$$

$$R_B M_n + Z \xrightarrow{k_z} P_B M_n + Z\bullet \quad (26)$$

$$R_C M_n + Z \xrightarrow{2k_z} R_A M_m + Z\bullet \quad (27)$$

$$Z\bullet + Z\bullet \xrightarrow{k_z} Z \quad (28)$$

In Equation (1–28), I is the bifunctional peroxide initiator, R_A is an initiation radical, R_B is a radical with an undecomposed peroxide group, Z and M are the inhibitor and monomer molecule, respectively. The remaining species in the reaction mechanism are described in Table 1. All reactions are assumed to occur in both the monomeric ($j = 1$) and polymeric ($j = 2$) phases.

2.2. Distribution of Components in Different Stages

As usual in kinetic modeling, some assumptions are necessary for development of the mass balances in the different process stages:

i) All phases are in equilibrium throughout the reaction. In the case of the monomer, this implies that:

$$\hat{f}_{m,1} = \hat{f}_{m,2} = \hat{f}_{m,v} = \hat{f}_{m,aq} \quad (29)$$

where $\hat{f}_{m,i}$ is the fugacity of the monomer in phase i, $i = 1, 2, v, aq$;

ii) the initiator concentration is the same in the monomeric and polymeric phases;

Table 1. Description of the macromolecular chains.

Species	Description
$R_A\ M_n$	Living macroradicals of length n
$R_B\ M_n$	Living reinitiating macroradicals of length n (containing one undecomposed peroxide group)
$R_C\ M_n$	Living bifunctional macroradicals of length n
$P_{A,n}$	Dead polymers of length n
$P_B\ M_n$	Reinitiating polymers of length n (containing one undecomposed peroxide group)
$P_{2B}\ M_n$	Reinitiating polymers of length n (containing two undecomposed peroxide groups)
$Z\bullet$	Primary radicals from inhibitor molecules

iii) the vapor phase is an ideal mixture, consisting of water and vinyl chloride;
iv) the solubility of VCM in the polymeric phase can be calculated using the Flory–Huggins theory for polymer solutions;
v) the polymerization takes place in three stages. The first stage comprises three phases (aqueous, gaseous, and monomeric phases) and ends when the limit of solubility of the polymer in the monomeric phase is reached. The second stage includes four phases (aqueous, gaseous, monomeric, and polymeric phases) and ends when the monomeric phase is consumed. The third and final stage includes three phases: aqueous, gaseous, and polymeric phases.
vi) the solubility of polymer in the monomeric phase is 0.5 wt% at the analyzed reaction temperature.[42]

The distribution of the components among the various phases in the reactor is very important for the complete understanding of the process. The composition of each phase is calculated with the aid of coupled thermodynamic correlations and mass balance equations.

At any stage, the total mass in the reactor can be calculated with Equation (30)

$$M_t = M_1 + M_2 + M_v + M_{aq} \tag{30}$$

where M_1 is the total mass of the monomeric phase, M_2 is the total mass of the polymeric phase, M_v is the total mass of vapor, and M_{aq} is the total mass of the aqueous phase. The total amount of VCM distributed among the phases is:

$$M_m = M_{m,1} + M_{m,2} + M_{m,v} + M_{m,aq} \tag{31}$$

where the variables M_m, $M_{m,1}$, $M_{m,2}$, $M_{m,v}$, $M_{m,aq}$, are, respectively, the mass of unreacted VCM, and the masses of VCM in the monomeric, polymeric, vapor, and aqueous phases.

The gas phase contains monomer and water; the monomeric phase contains VCM, initiator, radicals, and polymer, while the aqueous phase contains water and monomer. The mass of VCM available for polymerization can be calculated with Equation (32)

$$M_m = M_{m,o}(1 - X) \tag{32}$$

where X is the monomer conversion and $M_{m,o}$ is the total mass of vinyl chloride at beginning of process. The polymer solubilized in the monomeric phase, M_p, and the total mass of the monomeric phase, M_1, are calculated as:

$$M_p = M_{m,o}X \tag{33}$$

$$M_1 = \left(\frac{M_t - M_{aq} - \rho_v(V_r + M_p/\rho_m - M_p/\rho_p - M_{aq}/\rho_{aq})}{1 - \rho_v/\rho_m}\right) \tag{34}$$

In order to calculate the VCM mass in the aqueous phase, it is necessary to describe the VCM solubility in water, $k_{sol,m}$ (w/w). A least squares fit of experimental data[43] led to Equation (35):

$$\begin{aligned} k_{sol,m} = {} & 9.11 \times 10^{-7}(T_r - 273.15)^3 \\ & -2.22 \times 10^{-5}(T_r - 273.15)^2 \\ & -3.5 \times 10^{3}(T_r - 273.15) + 0.9913 \end{aligned} \tag{35}$$

where T_r is the reaction temperature. Once the solubility is calculated, the mass of VCM in the aqueous phase is found as:

$$M_{m,aq} = k_{sol,m}\left(\frac{P_t}{P_m^{sat}}\right)M_{w,aq} \tag{36}$$

where P_t is the total pressure, P_m^{sat} is the monomer vapor pressure and $\overline{M}_{w,aq}$ is the mass of water in the aqueous phase. After some algebraic manipulations, one can find the total mass of the aqueous phase according to Equation (37)

$$M_{aq} = \rho_w\left(\frac{\omega_{w,v}\rho_v\rho_m\rho_p V_r - \omega_{w,v}\rho_v\rho_m M_p - M_w\rho_m\rho_p + M_w\omega_{m,v}\rho_v\rho_p - M_m\omega_{w,v}\rho_v\rho_p}{(\omega_{w,a}\rho_p)(\omega_{w,v}\rho_v\rho_m - \rho_w\rho_m + \omega_{m,v}\rho_w\rho_m)}\right) \tag{37}$$

2.2.1. First stage: $0 < X < X_P$

The first stage of VCM suspension polymerizations is characterized by the absence of the polymeric phase. Once the solubility limit of polymer in the monomeric phase is reached, a new phase appears and the stage ends.

where ω is the mass fraction of each component in the respective phase.

As the vapor phase is considered an ideal gas mixture, the fugacity of each component in the gas mixture is equal to its partial pressure

$$\hat{f}_{m,v} = P_{m,v} \quad \text{and} \quad \hat{f}_{w,v} = P_{w,v} \tag{38}$$

Thus, one can calculate the total system pressure as the sum of the partial pressures of water and VCM, respectively.

$$P_t = P_{m,v} + P_{w,v} \tag{39}$$

Finally, it is possible to calculate the density of the vapor phase as:

$$\rho_v = \frac{P_t \overline{MM}_v}{RT_r} \tag{40}$$

where $\overline{MM}_v$ is the molecular weight of the mixture in the vapor phase and R is the gas constant.

2.2.2. Second Stage: $X_p < X < X_f$

In this stage, the polymer phase is formed by precipitation of polymer and macroradicals. Thus, four phases are present in the reactor. The total mass of the aqueous phase and the density of the vapor phase can be calculated as described before for the first stage. The volume of the vapor phase, V_v, can be calculated as:

$$V_v = V_r - V_{aq} - V_1 - V_2 \tag{41}$$

where V_r, V_{aq}, V_1, and V_2 are the volumes of the reactor and the aqueous, monomeric, and polymeric phases, respectively.

It is possible to calculate the mass of the vapor phase from the mass balance of components, as indicated in Equation (42)

$$M_v = \rho_v \left[V_r - \left(\frac{\omega_{w,aq} M_{aq}}{\rho_w} - \frac{\omega_{m,aq} M_{aq}}{\rho_m} \right) - \left(\frac{\omega_{m,1} M_1}{\rho_m} - \frac{\omega_{p,1} M_2}{\rho_p} \right) - \left(\frac{\omega_{m,2} M_2}{\rho_m} - \frac{\omega_{p,2} M_2}{\rho_p} \right) \right] \tag{42}$$

As the polymerization proceeds, the mass of the polymeric phase increases at the expense of the monomeric phase. The composition of the polymeric phase can be calculated with help of the Flory–Huggins equation,[44] as described elsewhere.[44–46] The monomer activity, a_m, can be calculated from the Flory–Huggins equation as:

$$\ln(a_m) = \ln(1 - \phi_p) + \left(1 - \frac{1}{r}\right)\phi_p + \chi_{FH}\phi_p^2 \tag{43}$$

The detailed calculation of the r factor, Flory–Huggins interaction parameter, χ, and the monomer activity is presented in the Appendix. From the volume fraction of polymer, $\phi_{p,2}$, the mass fraction of polymer in the polymeric phase ($\omega_{p,2}$) can calculated according to Equation (45)

$$\omega_{p,2} = \frac{\phi_{p,2}\rho_p}{\phi_{p,2}\rho_p + (1 - \phi_{p,2})\rho_m} \tag{44}$$

The end of the second stage is reached at a critical conversion X_f, where the monomeric phase disappears. Some equations for X_f are reported in the literature,[18–22] but none of them are used here. In the present model, the disappearance of the monomeric phase is monitored with the mass balance equations.

2.2.3. Third Stage: $X_f < X < 1.0$

As mentioned above, the third stage is characterized by the presence of three phases: aqueous, vapor, and polymeric phases. The mass distribution of VCM among these phases is shown in Equation (45–47)

$$M_{m,1} = 0;\ M_m(1 - X) = M_{m,aq} + M_{m,v} + M_{m,2} \tag{45}$$

$$M_{m,2} = \left(\frac{M_t + M_{aq} + \rho_v(V_r - (M_{aq}/\rho_w)) - M_p(1 - (\rho_v/\rho_p))}{(1 - (\rho_v/\rho_m))} \right) \tag{46}$$

$$M_v = M_t - M_{aq} - M_2;\ M_{m,v} = \omega_{m,v} M_v \tag{47}$$

2.2.4. Gel Effect

The reaction rate in the suspension polymerization system can be diffusion-controlled (gel effect). There are many models available in the literature to describe this effect.[51–53] These methods account for the gel effect by reducing the termination constant as the conversion and viscosity increase during the reaction.[54] The initiation, propagation, and chain transfer rate constants are also affected by diffusion, related to the *cage effect* and *glass effect*, respectively.

The gel effect has been associated to the decrease of the free volume,[54] which is defined as the volume of void in the reaction mass, where the molecular motion and diffusion take place. According to the free-volume theory,[55] Equation (48) and (49) apply:

$$V_{f,m} = (0.025 + \alpha_m(T - T_{gm}))\phi_m \tag{48}$$

$$V_{f,p} = (0.025 + \alpha_p(T - T_{gp}))\phi_p \tag{49}$$

$$V_{f,i} = V_{f,m} + V_{f,p} \tag{50}$$

where $V_{f,m}$ is the relative contribution of the monomer to the free volume, $V_{f,p}$ is the relative contribution of the polymer to the free volume, T_{gm} and T_{gp} are the glass transition temperature of the monomer and polymer, respectively. The total free volume fraction of the organic phase ($V_{f,i}$) in phase i is defined as the sum of the individual contributions of the monomer and the polymer.

To represent the diffusion effect (gel effect) on the termination rate constant of phase i in all stages, the following equations apply

$$k_{t,1} = k_t \tag{51}$$

$$k_{t,2} = k_t \exp\left[-\mathbf{A}\left(\frac{1}{V_{f,i}} - \frac{1}{V_{f,c}}\right)\right] \tag{52}$$

where V_{fc} is defined as the critical free volume fraction at which the monomer phase is completely consumed at the end of second stage. A value of 80% $V_{f,i}$ was used for V_{fc} in the present paper, as reported by Xie et al.[18]

The kinetic rate constants for propagation and chain transfer to monomer, as well as the initiation efficiency, are also affected by the diffusion effects. The effect can be described using the following equations:

$$k_{p,2} = k_p \exp\left[-\mathbf{B}\left(\frac{1}{V_{f,i}} - \frac{1}{V_{fv}}\right)\right] \tag{53}$$

$$k_{tr,2} = k_{tr} \exp\left[-\mathbf{C}\left(\frac{1}{V_{f,i}} - \frac{1}{V_{fv}}\right)\right] \tag{54}$$

$$f_i = f_{i,o} \exp\left(\frac{1}{V_{f,i}} - \frac{1}{V_{fv}}\right) \tag{55}$$

where **A**, **B**, and **C** are temperature dependent constants that have been estimated from experimental data;[22] V_{fv} is the critical volume fraction for the glass effect at the end of the second stage, which means, $V_{fv} = V_{f,p}$; $f_{i,o}$ is the initial efficiency determined for each type of initiator.

In this work, it is assumed that a fraction of the radicals generated by the initiator decomposition can be consumed by side reactions instead of producing macromolecular chains. Such radicals can be influenced by the cage effect,[53] as well as other factors, meaning that an efficiency of initiation f must also be calculated during the reaction course.

2.2.5. Mass Balances

Mass balances for monomer, polymer chains, macroradicals, and radicals present in the free-radical suspension polymerization of vinyl chloride are described below, taking into account all the hypotheses discussed previously.

- Initiator

$$\frac{1}{V_j}\frac{d[I]}{dt} = -\sum_{j=1}^{2} 2k_{d,j}[I]_j \tag{56}$$

- Primary radicals without undecomposed peroxide group

$$\frac{1}{V_j}\frac{d[R_A]}{dt} = \sum_{j=1}^{2}\left\{2f_{A,j}k_{d,j}[I]_j + f_{dr,j}k_{dr,j}\sum_{m=1}^{\infty}[R_B M_m]_j - k_{iA,j}[M]_j[R_A]_j + f_{dp,j}k_{dp,j}\left(\sum_{m=1}^{\infty}[P_B M_m]_j + 2\sum_{m=1}^{\infty}[P_{2B} M_m]_j\right)\right\} \tag{57}$$

- Primary radicals with undecomposed peroxide group

$$\frac{1}{V_j}\frac{d[R_B]}{dt} = \sum_{j=1}^{2}\left\{2f_{B,j}k_{d,j}[I]_j - k_{iB}[M]_j[R_B]_j\right\} \tag{58}$$

- Vinyl chloride

$$\frac{1}{V_j}\frac{d[M]_j}{dt} = -k_{iA,j}[R_A]_j[M]_j - k_{iB,j}[R_B]_j[M]_j - k_{p,j}[M]_j([R_A M_n]_j + [R_B M_n]_j) - 2k_{p,j}[M]_j[R_C M_n]_j - k_{tr,j}[M]_j([R_A M_n]_j + [R_B M_n]_j) - 2k_{tr,j}[M]_j[R_C M_n]_j \tag{59}$$

- Inhibitor

$$\frac{1}{V_j}\frac{d[Z]_j}{dt} = -k_{Z,j}[Z]_j\sum_{n=1}^{\infty}([R_A M_n]_j + [R_B M_n]_j + 2[R_C M_n]_j) \tag{60}$$

- Macroradicals (length n) without undecomposed peroxide group

$$\begin{aligned}\frac{1}{V_j}\frac{d[R_A M_n]_j}{dt} &= (k_{p,j}[R_A]_j[M]_j + k_{tr,j}[M]_j\sum_{m=1}^{\infty}[R_A M_m]_j + k_{tr,j}[M]_j\sum_{m=1}^{\infty}[R_B M_m]_j \\ &+2k_{tr,j}[M]_j\sum_{m=1}^{\infty}[R_C M_m]_j)\delta(n-1) + 2k_{z,j}[Z]_j\sum_{m=1}^{\infty}[R_C M_m]_j \\ &+f_{dp,j}k_{dp,j}[P_B M_n]_j + (1-f_{dr,j})k_{dr,j}[R_B M_n]_j + k_{p,j}[M]_j[R_A M_{n-1}]_j \\ &+2k_{tr,j}[M]_j[R_C M_n]_j + 2k_{tc,j}\sum_{m=1}^{n-1}[R_A M_m]_j[R_C M_{n-m}]_j \\ &+2k_{td,j}[R_C M_n]_j\left(\sum_{m=1}^{\infty}[R_A M_m]_j + \sum_{m=1}^{\infty}[R_B M_m]_j + 2\sum_{m=1}^{\infty}[R_C M_m]_j\right) \\ &-k_{tr,j}[M]_j[R_A M_n]_j - k_{p,j}[M]_j[R_A M_n]_j - 2k_{tc,j}[R_A M_n]_j\sum_{m=1}^{\infty}[R_C M_m]_j \\ &-k_{tc,j}[R_A M_n]_j\left(\sum_{m=1}^{\infty}[R_A M_m]_j + \sum_{m=1}^{\infty}[R_B M_m]_j\right) - 2k_{td,j}[R_A M_n]_j\sum_{m=1}^{\infty}[R_C M_m]_j \\ &-k_{td,j}[R_A M_n]_j\left(\sum_{m=1}^{\infty}[R_A M_m]_j + \sum_{m=1}^{\infty}[R_B M_m]_j\right) - k_{Z,j}[Z]_j[R_A M_n]_j\end{aligned} \tag{61}$$

- Macroradicals (length n) with undecomposed peroxide group

$$\begin{aligned}\frac{1}{V_j}\frac{d[R_B M_n]_j}{dt} &= k_{p,j}[R_B]_j[M]_j\delta(n-1) + k_{p,j}[M]_j[R_B M_{n-1}]_j + 2f_{dp,j}k_{dp,j}[P_{2B} M_n]_j \\ &+2k_{tc,j}\sum_{m=1}^{n-1}[R_B M_m]_j[R_C M_{n-m}]_j - k_{dr,j}[R_B M_n]_j - k_{tr,j}[M]_j[R_B M_n]_j \\ &-k_{p,j}[M]_j[R_B M_n]_j - k_{z,j}[Z]_j[R_B M_n]_j - 2k_{tc,j}[R_B M_n]_j\sum_{m=1}^{\infty}[R_C M_m]_j \\ &-k_{tc,j}[R_B M_n]_j\left(\sum_{m=1}^{\infty}[R_A M_m]_j + \sum_{m=1}^{\infty}[R_B M_m]_j\right) - 2k_{td,j}[R_B M_n]_j\sum_{m=1}^{\infty}[R_C M_m]_j \\ &-k_{td,j}[R_B M_n]_j\left(\sum_{m=1}^{\infty}[R_A M_m]_j + \sum_{m=1}^{\infty}[R_B M_m]_j\right)\end{aligned} \tag{62}$$

- Macroradicals (length n) with two terminal peroxide groups

$$\begin{aligned}\frac{1}{V_j}\frac{d[R_C M_n]_j}{dt} &= 2k_{p,j}[R_C]_j[M]_j\delta(n-1) + f_{dr,j}k_{dr,j}[R_B M_n]_j + 2k_{tc,j}\sum_{m=1}^{n-1}[R_C M_m]_j[R_C M_{n-m}]_j \\ &-2k_{p,j}[M]_j[R_C M_n]_j - 2k_{tr,j}[M]_j[R_C M_n]_j - 2k_{z,j}[Z]_j[R_C M_n]_j \\ &-4k_{tc,j}[R_C M_n]_j\sum_{m=1}^{\infty}[R_C M_m]_j - 2k_{tc,j}[R_C M_n]_j\left(\sum_{m=1}^{\infty}[R_A M_m]_j + \sum_{m=1}^{\infty}[R_B M_m]_j\right) \\ &-4k_{td,j}[R_C M_n]_j\sum_{m=1}^{\infty}[R_C M_m]_j - 2k_{td,j}[R_C M_n]_j\left(\sum_{m=1}^{\infty}[R_A M_m]_j + \sum_{m=1}^{\infty}[R_B M_m]_j\right)\end{aligned} \tag{63}$$

- Dead polymer chains (length n)

$$\begin{aligned}\frac{1}{V_j}\frac{d[P_{A,n}]_j}{dt} &= k_{tr,j}[M]_j[R_A M_n]_j + (1-f_{dp,j})k_{dp,j}[P_B M_n]_j + \frac{1}{2}k_{tc,j}\sum_{m=1}^{n-1}[R_A M_m]_j[R_A M_{n-m}]_j \\ &+k_{td,j}[R_A M_n]_j\left(\sum_{m=1}^{\infty}[R_A M_m]_j + \sum_{m=1}^{\infty}[R_B M_m]_j\right) + 2k_{td,j}[R_A M_n]_j\sum_{m=1}^{\infty}[R_C M_m]_j \\ &+k_{z,j}[Z]_j[R_A M_n]_j\end{aligned} \tag{64}$$

- Inactive polymer chains with undecomposed peroxide group (length n)

$$\frac{1}{V_j}\frac{\mathrm{d}\,[P_B M_n]_j}{\mathrm{d}t} = k_{tr,j}[M]_j[R_B M_n]_j + (1-f_{dp,j})k_{dp,j}[P_{2B}M_n]_j + k_{tc,j}\sum_{m=1}^{n-1}[R_A M_m]_j[R_B M_{n-m}]_j + k_{td,j}[R_B M_n]_j\left(\sum_{m=1}^{\infty}[R_A M_m]_j + \sum_{m=1}^{\infty}[R_B M_m]_j\right) + 2k_{td,j}[R_B M_n]_j\sum_{m=1}^{\infty}[R_C M_m]_j + k_{z,j}[Z]_j[R_B M_n]_j - k_{dp,j}[P_B M_n]_j \quad (65)$$

- Inactive polymer chains with two terminal peroxide groups (length n)

$$\frac{1}{V_j}\frac{\mathrm{d}\,[P_{2B} M_n]_j}{\mathrm{d}t} = \frac{1}{2}k_{tc,j}\sum_{m=1}^{n-1}[R_B M_m]_j[R_B M_{n-m}]_j - 2k_{dp,j}[P_{2B}M_n]_j \quad (66)$$

In Equation (61–66), $\delta(n-1)$ is the Kronecker delta, where $\delta(n-1)=1$ for $n=1$ and 0 for $n \neq 1$, and subscript j represents each of the reaction phases.

2.3. The Method of Moments

The produced polymer may be characterized through its number average molecular weight ($\overline{M}_n$), mass average molecular weight ($\overline{M}_w$), and molar-mass dispersity ($Đ_M$). These properties can be calculated with the aid of the method of moments.[23] Even though it is common to apply the quasi-steady-state approximation (QSSA) when modeling free radical polymerizations,[4,18–21] the QSSA was not used in the present work. Equation (67) and (68) define the kth-order moment of the chain length distributions of the living macroradicals and the polymers, respectively:

$$[\lambda_{\tau,k}] = \sum_{n=i}^{\infty} n^k [R_\tau M_n], \quad k = 0,1,2 \quad \tau = A, B, C \quad (67)$$

$$[\mu_{\varsigma,k}] = \sum_{n=i}^{\infty} n^k [P_{\varsigma,n}], \quad k = 0,1,2 \quad \varsigma = A, B, 2B \quad (68)$$

where k is the order of the moment, $[R_\tau M_n]$, $\tau = A, B, C$ are the concentrations of living macroradicals of size n, and $[P_{\varsigma,n}]$, $\varsigma = A, B, 2B$, are the concentrations of dormant or dead polymer chains of size n. The description of all species is summarized in Table 1.

The first few moments of the size distributions can be associated directly with physical quantities. For example, the 0th-order moments correspond to the total molar concentration of any given species, while the first-order moment can be associated to the total number of monomers incorporated into a type of chain. The second order moments may be associated to the heterogeneity of the MWD.[23]

After applying the definitions of each type of moment to the mass balance equations, the following moment balance equations can be found:

- Rate equations for the kth-order moment of the size distribution of live polymer chains (without undecomposed peroxide group)

$$\begin{aligned}\frac{1}{V_j}\frac{\mathrm{d}\,[\lambda_{A,k}]_j}{\mathrm{d}t} &= k_{p,j}[R_A]_j[M]_j + f_{dp,j}k_{dp,j}[\mu_{B,k}]_j + (1-f_{dr,j})k_{dr,j}[\lambda_{B,k}]_j \\ &+ k_{p,j}[M]_j\left[\sum_{r=0}^{k}\binom{k}{r}[\lambda_{A,r}]_j - [\lambda_{A,k}]_j\right] + 2k_{tc,j}\left[\sum_{r=0}^{k}\binom{k}{r}[\lambda_{A,r}]_j[\lambda_{C,k-r}]_j\right] \\ &+ k_{tr,j}[M]_j([\lambda_{A,0}]_j + [\lambda_{B,0}]_j + 2[\lambda_{C,0}]_j) + k_{z,j}[Z]_j(2[\lambda_{C,k}]_j - [\lambda_{A,k}]_j) \\ &+ 2k_{td,j}[\lambda_{C,k}]_j([\lambda_{A,0}]_j + [\lambda_{B,0}]_j + 2[\lambda_{C,0}]_j) + k_{tr,j}[M]_j(2[\lambda_{C,k}]_j - [\lambda_{A,k}]_j) \\ &- k_{tc,j}[\lambda_{A,k}]_j([\lambda_{A,0}]_j + [\lambda_{B,0}]_j + 2[\lambda_{C,0}]_j) \\ &- k_{td,j}[\lambda_{A,k}]_j([\lambda_{A,0}]_j + [\lambda_{B,0}]_j + 2[\lambda_{C,0}]_j)\end{aligned} \quad (69)$$

- Rate equations for the kth-order moment of the size distribution of live polymer chains (with undecomposed peroxide group)

$$\frac{1}{V_j}\frac{\mathrm{d}[\lambda_{\mathrm{B},k}]_j}{\mathrm{d}t} = k_{\mathrm{p},j}[R_{\mathrm{B}}]_j[M]_j + 2f_{\mathrm{dp},j}k_{\mathrm{dp},j}[\mu_{2\mathrm{B},k}]_j + k_{\mathrm{p},j}[M]_j\left[\sum_{r=0}^{k}\binom{k}{r}[\lambda_{\mathrm{B},r}]_j - [\lambda_{\mathrm{B},k}]_j\right] + 2k_{\mathrm{tc},j}\left[\sum_{r=0}^{k}\binom{k}{r}[\lambda_{\mathrm{B},r}]_j[\lambda_{\mathrm{C},k-r}]_j\right]$$
$$- k_{\mathrm{tr},j}[M]_j[\lambda_{\mathrm{B},k}]_j - k_{z,j}[Z]_j[\lambda_{\mathrm{B},k}]_j - k_{\mathrm{dr},j}[\lambda_{\mathrm{B},k}]_j - k_{\mathrm{tc},j}[\lambda_{\mathrm{B},k}]_j([\lambda_{\mathrm{A},0}]_j + [\lambda_{\mathrm{B},0}]_j + 2[\lambda_{\mathrm{C},0}]_j)$$
$$- k_{\mathrm{td},j}[\lambda_{\mathrm{B},k}]_j([\lambda_{\mathrm{A},0}]_j + [\lambda_{\mathrm{B},0}]_j + 2[\lambda_{\mathrm{C},0}]_j) \tag{70}$$

- Rate equations for the kth-order moment of the size distribution of live polymer chains (with two terminal peroxide groups)

$$\frac{1}{V_j}\frac{\mathrm{d}[\lambda_{\mathrm{C},k}]_j}{\mathrm{d}t} = 2k_{\mathrm{p},j}[R_{\mathrm{C}}]_j[M]_j + f_{\mathrm{dr},j}k_{\mathrm{dr},j}[\lambda_{\mathrm{B},k}]_j + k_{\mathrm{p},j}[M]_j\left[\sum_{r=0}^{k}\binom{k}{r}[\lambda_{\mathrm{C},r}]_j - [\lambda_{\mathrm{C},k}]_j\right] + 2k_{\mathrm{tc},j}\left[\sum_{r=0}^{k}\binom{k}{r}[\lambda_{\mathrm{C},r}]_j[\lambda_{\mathrm{C},k-r}]_j\right]$$
$$- 2k_{\mathrm{tr},j}[M]_j[\lambda_{\mathrm{C},k}]_j - 2k_{z,j}[Z]_j[\lambda_{\mathrm{C},k}]_j - 2k_{\mathrm{tc},j}[\lambda_{\mathrm{C},k}]_j([\lambda_{\mathrm{A},0}]_j + [\lambda_{\mathrm{B},0}]_j + 2[\lambda_{\mathrm{C},0}]_j)$$
$$- 2k_{\mathrm{td},j}[\lambda_{\mathrm{C},k}]_j([\lambda_{\mathrm{A},0}]_j + [\lambda_{\mathrm{B},0}]_j + 2[\lambda_{\mathrm{C},0}]_j) \tag{71}$$

- Rate equations for the kth-order moment of the size distribution of dead polymer chains

$$\frac{1}{V_j}\frac{\mathrm{d}[\mu_{\mathrm{A},k}]_j}{\mathrm{d}t} = k_{\mathrm{tr},j}[M]_j[\lambda_{\mathrm{A},k}]_j + (1-f_{\mathrm{dp},j})k_{\mathrm{dp},j}[\lambda_{\mathrm{B},k}]_j + k_{z,j}[Z]_j[\lambda_{\mathrm{A},k}]_j + k_{\mathrm{td},j}[\lambda_{\mathrm{A},k}]_j([\lambda_{\mathrm{A},0}]_j + [\lambda_{\mathrm{B},0}]_j + 2[\lambda_{\mathrm{C},0}]_j)$$
$$+ \frac{1}{2}k_{\mathrm{tc},j}\left[\sum_{r=0}^{k}\binom{k}{r}[\lambda_{\mathrm{A},r}]_j[\lambda_{\mathrm{A},k-r}]_j\right] \tag{72}$$

- Rate equations for the kth-order moment of the size distribution of dormant polymer chains (with undecomposed peroxide group – length n)

$$\frac{1}{V_j}\frac{\mathrm{d}[\mu_{\mathrm{B},k}]_j}{\mathrm{d}t} = k_{\mathrm{tr},j}[M]_j[\lambda_{\mathrm{B},k}]_j + 2(1-f_{\mathrm{dp},j})k_{\mathrm{dp},j}[\mu_{2\mathrm{B},k}]_j + k_{z,j}[Z]_j[\lambda_{\mathrm{B},k}]_j + k_{\mathrm{td},j}[\lambda_{\mathrm{B},k}]_j([\lambda_{\mathrm{A},0}]_j + [\lambda_{\mathrm{B},0}]_j + 2[\lambda_{\mathrm{C},0}]_j)$$
$$+ k_{\mathrm{tc},j}\left[\sum_{r=0}^{k}\binom{k}{r}[\lambda_{\mathrm{A},r}]_j[\lambda_{\mathrm{B},k-r}]_j\right] - k_{\mathrm{dp},j}[\mu_{\mathrm{B},k}]_j \tag{73}$$

- Rate equations for the kth-order moment of the size distribution of dormant polymer chains (two terminal peroxide groups)

$$\frac{1}{V_j}\frac{\mathrm{d}[\mu_{2\mathrm{B},k}]_j}{\mathrm{d}t} = \frac{1}{2}k_{\mathrm{tc},j}\left[\sum_{r=0}^{k}\binom{k}{r}[\lambda_{\mathrm{B},r}]_j[\lambda_{\mathrm{B},k-r}]_j\right] - 2k_{\mathrm{dp},j}[\mu_{2\mathrm{B},k}]_j \tag{74}$$

The average molecular weights and molar-mass dispersity ($Đ_{\mathrm{M}}$) were calculated according to the following equations:

$$\overline{M}_{\mathrm{w}} = \frac{\sum_{j=1}^{2}\left([\lambda_{\mathrm{A},2}]_j + [\lambda_{\mathrm{B},2}]_j + [\lambda_{\mathrm{C},2}]_j + [\mu_{\mathrm{A},2}]_j + [\mu_{\mathrm{B},2}]_j + [\mu_{2\mathrm{B},2}]_j\right)}{\sum_{j=1}^{2}\left([\lambda_{\mathrm{A},1}]_j + [\lambda_{\mathrm{B},1}]_j + [\lambda_{\mathrm{C},1}]_j + [\mu_{\mathrm{A},1}]_j + [\mu_{\mathrm{B},1}]_j + [\mu_{2\mathrm{B},1}]_j\right)} \times MM_{\mathrm{m}} \tag{75}$$

$$\overline{M}_{\mathrm{n}} = \frac{\sum_{j=1}^{2}\left([\lambda_{\mathrm{A},1}]_j + [\lambda_{\mathrm{B},1}]_j + [\lambda_{\mathrm{C},1}]_j + [\mu_{\mathrm{A},1}]_j + [\mu_{\mathrm{B},1}]_j + [\mu_{2\mathrm{B},1}]_j\right)}{\sum_{j=1}^{2}\left([\lambda_{\mathrm{A},0}]_j + [\lambda_{\mathrm{B},0}]_j + [\lambda_{\mathrm{C},0}]_j + [\mu_{\mathrm{A},0}]_j + [\mu_{\mathrm{B},0}]_j + [\mu_{2\mathrm{B},0}]_j\right)} \times MM_{\mathrm{m}} \tag{76}$$

$$Đ_{\mathrm{M}} = \frac{\overline{M}_{\mathrm{w}}}{\overline{M}_{\mathrm{n}}} \tag{77}$$

where $\overline{M}_{\mathrm{n}}$ and $\overline{M}_{\mathrm{w}}$ are the overall $\overline{M}_{\mathrm{n}}$ and $\overline{M}_{\mathrm{w}}$ values of the polymer resin when all chain populations are considered simultaneously.

Conversion is calculated according to the equation below.

$$X(\%) = \frac{(m(0)_{\mathrm{m}} - m(t)_{\mathrm{m}})}{m(0)_{\mathrm{m}}} \times 100 \tag{78}$$

where $m(0)_{\mathrm{m}}$ is the total mass of VCM at time zero and $m(t)_{\mathrm{m}}$ is the remaining mass of VCM at time t.

2.4. Molecular Weight Distribution (MWD)

The probability generating function (pgf) technique is used here to calculate the MWD of the polymer resin and of the individual populations of polymer chains resulting from the VCM free radical suspension polymerization performed with the bifunctional initiator. The pgf method has been successfully employed for modeling the MWD of different free radical polymerization systems, including non-isothermal operation, complex kinetic mechanisms and branched polymers.[8,27,37,38] Some of these systems include the peroxide modification of polyethylenes[56] and polypropylenes,[57] styrene polymerizations performed with bifunctional initiators[8] and high-pressure ethylene polymerizations performed in tubular reactors.[58]

The pgf is a transform on a probability distribution $p_l(n)$ defined as

$$\phi_l(z) = \sum_{n=0}^{\infty} z^n p_l(n) \tag{79}$$

where z is the transformed variable, $0 \le z \le 1$, and $\phi_l(z)$ is the probability generating function associated to the distribution $p_l(n)$. As used in this work, z is real, and the pgf is a continuous, convex, increasing, bound real function that may take values between 0 and 1.[59] In this work, two distributions were used: the number distribution ($l = 0$), corresponding to a MWD expressed as number fraction versus molecular weight, and the mass distribution ($l = 1$), corresponding to MWD expressed as mass fraction versus molecular weight. Since radicals and polymers have distributions of length, different pgf's were defined for each of them. The functions $\phi_{A,l,j}(z)$, $\phi_{B,l,j}(z)$, $\phi_{C,l,j}(z)$, $l = 0,1$, $j = 1, 2$ are pgf's corresponding to radicals of type A, B or C, associated to number or mass distributions in either the polymeric ($j = 1$) or monomeric ($j = 2$) phases. Similarly, the functions $\psi_{\mathrm{A},l,j}(z)$, $\psi_{\mathrm{B},l,j}(z)$, $\psi_{2\mathrm{B},l,j}(z)$ $\phi_{\mathrm{A},l,j}(z)$, $\phi_{\mathrm{B},l,j}(z)$, $\phi_{\mathrm{C},l,j}(z)$, $l = 0,1$, $j = 1$, 2, are associated to the number or mass distributions of dormant or dead polymers in either of the monomeric or polymeric phases.

In order to apply the pgf transform to the mass balances, the general method consists in multiplying the mass balance equations by $n^a z^n$, $a = 0$, 1, and adding up over all possible chain lengths n. The result is reorganized in terms of the different pgf's and moments of the distributions. The procedure is simplified by the use of the pgf Transform table previously developed by Asteasuain et al.[37,38] After using it on the mass balances corresponding to this work, Equation (80–85) can be obtained as a result.

2.4.1. pgf of macroradicals

$$\begin{aligned}\frac{1}{V_j}\frac{\mathrm{d}((\lambda_{\mathrm{A},l}\theta_{\mathrm{A},l}(z))_j V_j)}{\mathrm{d}t} &= k_{i\mathrm{A},j} z [R_{\mathrm{A}}]_j [M]_j + k_{\mathrm{tr},j} z [M]_j ([\lambda_{\mathrm{A},0}]_j + [\lambda_{\mathrm{B},0}]_j + 2[\lambda_{\mathrm{C},0}]_j) + k_{\mathrm{tr},j}[M]_j (2(\lambda_{\mathrm{C},l}\theta_{\mathrm{C},l}(z))_j - (\lambda_{\mathrm{A},l}\theta_{\mathrm{A},l}(z))_j) \\ &+ k_{\mathrm{z},j}[z]_j (2(\lambda_{\mathrm{C},l}\theta_{\mathrm{C},l}(z))_j - (\lambda_{\mathrm{A},l}\theta_{\mathrm{A},l}(z))_j) + k_{\mathrm{p},j} z [M]_j \sum_{r=0}^{l}\binom{l}{r}(\lambda_{\mathrm{A},r}\theta_{\mathrm{A},r}(z))_j - k_{\mathrm{p},j}[M]_j (\lambda_{\mathrm{A},l}\theta_{\mathrm{A},l}(z))_j \\ &+ 2k_{\mathrm{tc},j}\sum_{r=0}^{l}\binom{l}{r}(\lambda_{\mathrm{C},l-r}\theta_{\mathrm{C},l-r}(z))_j (\lambda_{\mathrm{A},r}\theta_{\mathrm{A},r}(z))_j + 2k_{\mathrm{td},j}(\lambda_{\mathrm{C},l}\theta_{\mathrm{C},l}(z))_j ([\lambda_{\mathrm{A},0}]_j + [\lambda_{\mathrm{B},0}]_j + 2[\lambda_{\mathrm{C},0}]_j) \\ &+ f_{\mathrm{dp},j} k_{\mathrm{dp},j}(\mu_{\mathrm{B},l}\psi_{\mathrm{B},l}(z))_j + (1 - f_{\mathrm{dr},j}) k_{\mathrm{dr},j}(\lambda_{\mathrm{B},l}\theta_{\mathrm{B},l}(z))_j - k_{\mathrm{tc},j}(\lambda_{\mathrm{A},l}\theta_{\mathrm{A},l}(z))_j ([\lambda_{\mathrm{A},0}]_j + [\lambda_{\mathrm{B},0}]_j + 2[\lambda_{\mathrm{C},0}]_j) \\ &- k_{\mathrm{td},j}(\lambda_{\mathrm{A},l}\theta_{\mathrm{A},l}(z))_j ([\lambda_{\mathrm{A},0}]_j + [\lambda_{\mathrm{B},0}]_j + 2[\lambda_{\mathrm{C},0}]_j)\end{aligned} \tag{80}$$

$$\frac{1}{V_j}\frac{\mathrm{d}((\lambda_{\mathrm{B},l}\theta_{\mathrm{B},l}(z))_jV_j)}{\mathrm{d}t} = k_{i\mathrm{B},j}z[R_\mathrm{B}]_j[M]_j + k_{\mathrm{p},j}z[M]_j\sum_{r=0}^{l}\binom{l}{r}(\lambda_{\mathrm{B},r}\theta_{\mathrm{B},r}(z))_j - k_{\mathrm{p},j}[M]_j(\lambda_{\mathrm{B},l}\theta_{\mathrm{B},l}(z))_j$$
$$+ 2k_{\mathrm{tc},j}\sum_{r=0}^{l}\binom{l}{r}(\lambda_{\mathrm{C},l-r}\theta_{\mathrm{C},l-r}(z))_j(\lambda_{\mathrm{B},r}\theta_{\mathrm{B},r}(z))_j + 2f_{\mathrm{dp},j}k_{\mathrm{dp},j}(\mu_{2\mathrm{B},l}\psi_{2\mathrm{B},l}(z))_j \quad (81)$$
$$- k_{\mathrm{tr},j}[M]_j(\lambda_{\mathrm{B},l}\theta_{\mathrm{B},l}(z))_j - k_{\mathrm{dr},j}(\lambda_{\mathrm{B},l}\theta_{\mathrm{B},l}(z))_j - k_{\mathrm{z},j}[z]_j(\lambda_{\mathrm{B},l}\theta_{\mathrm{B},l}(z))_j$$
$$- k_{\mathrm{tc},j}(\lambda_{\mathrm{B},l}\theta_{\mathrm{B},l}(z))_j([\lambda_{\mathrm{A},0}]_j + [\lambda_{\mathrm{B},0}]_j + 2[\lambda_{\mathrm{C},0}]_j) - k_{\mathrm{td},j}(\lambda_{\mathrm{B},l}\theta_{\mathrm{B},l}(z))_j([\lambda_{\mathrm{A},0}]_j + [\lambda_{\mathrm{B},0}]_j + 2[\lambda_{\mathrm{C},0}]_j)$$

$$\frac{1}{V_j}\frac{\mathrm{d}((\lambda_{\mathrm{C},l}\theta_{\mathrm{C},l}(z))_jV_j)}{\mathrm{d}t} = 2k_{i\mathrm{C},j}z[R_\mathrm{C}]_j[M]_j + 2k_{\mathrm{p},j}z[M]_j\sum_{r=0}^{l}\binom{l}{r}(\lambda_{\mathrm{C},r}\theta_{\mathrm{C},r}(z))_j - 2k_{\mathrm{p},j}[M]_j(\lambda_{\mathrm{C},l}\theta_{\mathrm{C},l}(z))_j$$
$$+f_{\mathrm{dr},j}k_{\mathrm{dr},j}(\lambda_{\mathrm{B},l}\theta_{\mathrm{B},l}(z))_j + 2k_{\mathrm{tc},j}\sum_{r=0}^{l}\binom{l}{r}(\lambda_{\mathrm{C},l-r}\theta_{\mathrm{C},l-r}(z))_j(\lambda_{\mathrm{C},r}\theta_{\mathrm{C},r}(z))_j \quad (82)$$
$$-2k_{\mathrm{tr},j}[M]_j(\lambda_{\mathrm{C},l}\theta_{\mathrm{C},l}(z))_j - 2k_{\mathrm{tc},j}(\lambda_{\mathrm{C},l}\theta_{\mathrm{C},l}(z))_j([\lambda_{\mathrm{A},0}]_j + [\lambda_{\mathrm{B},0}]_j + 2[\lambda_{\mathrm{C},0}]_j)$$
$$-2k_{\mathrm{td},j}(\lambda_{\mathrm{C},l}\theta_{\mathrm{C},l}(z))_j([\lambda_{\mathrm{A},0}]_j + [\lambda_{\mathrm{B},0}]_j + 2[\lambda_{\mathrm{C},0}]_j) - 2k_{\mathrm{z},j}[z]_j(\lambda_{\mathrm{C},l}\theta_{\mathrm{C},l}(z))_j$$

2.4.2. pgf of the permanent polymer

$$\frac{1}{V_j}\frac{\mathrm{d}((\mu_{\mathrm{A},l}\psi_{\mathrm{A},l}(z))_jV_j)}{\mathrm{d}t} = k_{\mathrm{tr},j}[M]_j(\lambda_{\mathrm{A},l}\theta_{\mathrm{A},l}(z))_j + \frac{1}{2}k_{\mathrm{tc},j}\sum_{r=0}^{l}\binom{l}{r}(\lambda_{\mathrm{A},l-r}\theta_{\mathrm{A},l-r}(z))_j(\lambda_{\mathrm{A},r}\theta_{\mathrm{A},r}(z))_j$$
$$+ k_{\mathrm{td},j}(\lambda_{\mathrm{A},l}\theta_{\mathrm{A},l}(z))_j([\lambda_{\mathrm{A},0}]_j + [\lambda_{\mathrm{B},0}]_j + 2[\lambda_{\mathrm{C},0}]_j) + (1-f_{\mathrm{dp},j})k_{\mathrm{dp},j}(\mu_{\mathrm{B},l}\psi_{\mathrm{B},l}(z))_j + k_{\mathrm{z},j}[z]_j(\lambda_{\mathrm{A},l}\theta_{\mathrm{A},l}(z))_j \quad (83)$$

2.4.3. pgf of temporary polymers

$$\frac{1}{V_j}\frac{\mathrm{d}((\mu_{\mathrm{B},l}\psi_{\mathrm{B},l}(z))_jV_j)}{\mathrm{d}t} = k_{\mathrm{tr},j}[M]_j(\lambda_{\mathrm{B},l}\theta_{\mathrm{B},l}(z))_j + k_{\mathrm{tc},j}\sum_{r=0}^{l}\binom{l}{r}(\lambda_{\mathrm{B},l-r}\theta_{\mathrm{B},l-r}(z))_j(\lambda_{\mathrm{A},r}\theta_{\mathrm{A},r}(z))_j$$
$$+ k_{\mathrm{td},j}(\lambda_{\mathrm{B},l}\theta_{\mathrm{B},l}(z))_j([\lambda_{\mathrm{A},0}]_j + [\lambda_{\mathrm{B},0}]_j + 2[\lambda_{\mathrm{C},0}]_j) + 2(1-f_{\mathrm{dp},j})k_{\mathrm{dp},j}(\mu_{2\mathrm{B},l}\psi_{2\mathrm{B},l}(z))_j \quad (84)$$
$$+ k_{\mathrm{z},j}[z]_j(\lambda_{\mathrm{B},l}\theta_{\mathrm{B},l}(z))_j - k_{\mathrm{dp},j}(\mu_{\mathrm{B},l}\psi_{\mathrm{B},l}(z))_j$$

$$\frac{1}{V_j}\frac{\mathrm{d}((\mu_{2\mathrm{B},l}\psi_{2\mathrm{B},l}(z))_jV_j)}{\mathrm{d}t} = \frac{1}{2}k_{\mathrm{tc},j}\sum_{r=0}^{l}\binom{l}{r}(\lambda_{\mathrm{B},l-r}\theta_{\mathrm{B},l-r}(z))_j(\lambda_{\mathrm{B},r}\theta_{\mathrm{B},r}(z))_j - 2k_{\mathrm{dp},j}(\mu_{2\mathrm{B},l}\psi_{2\mathrm{B},l}(z))_j \quad (85)$$

The pgf are not useful by themselves; they must be inverted in order to recover the different distributions. The inversion algorithm is composed of a set of algebraic equations that are solved together with the pgf equations and allow for the recovery of the MWDs from their corresponding pgf transforms. In previous works,[8,37,38] eight distinct numerical inversion methods appropriate for the inversion of pgf of MWDs were studied and the Papoulis inversion method can be recommended.[8,38]

2.5. Numerical Methodology

The model and all algorithms were implemented in Fortran 2003 code on a personal computer with an Intel 64 i7 Core processor, 8 Gb RAM and 1 Tb hard drive. All differential equations of this model were integrated simultaneously with the numerical integration package DIVPAG, which is included in the numerical packages IMSL Library 6.0.[60] The implicit BDF (*backward differentiation*) discretization method for the dynamic integration of sets of differential-algebraic equations was applied to the model. The numerical precision used in the integration of differential equations was always equal to 1.0×10^{-9}.

2.6. Model Parameters and Simulation Conditions

In order to validate the model developed in the present work, published experimental data were used.[22] To the

Table 2. Reaction conditions used in this study and implemented in the mathematical model.

T_r (°C)	I% (kg I/kg VCM)	H_2O % (kg_{H_2O}/kg_{VCM})
$T_{r1} = 45.0$	0.835	1.55
$T_{r2} = 54.5$	0.835	1.55
$T_{r3} = 56.5$	0.835	1.55
$T_{r4} = 50.0$	0.835	1.55
$T_{r5} = 50.0$	1.000	1.55
$T_{r6} = 50.0$	1.500	1.55
$T_{r7} = 50.0$	2.000	1.55

best of our knowledge these are the only published data on suspension polymerization of vinyl chloride using the bifunctional initiator DIPND. Once the model was validated, other reaction conditions were simulated and added in this study in order to assess the sensitivity of the model to the operation and design variables of industrial interest. Table 2 shows the reaction recipes used in the present study.

Since the published data[22] did not include the dimensions of the reactor, a set of dimensions that are consistent with published data for industrial reactors of 60 m^3 was used, as described in the literature.[61,62] All simulations were performed using the experimentally measured temperature profiles described in the previous study,[22] so that it was not necessary to include the energy balance in the simulation study.

The set of parameters and kinetic constants used for the development of this study are presented in Table 3, while the parameters required for the representation of the diffusive effect and thermodynamic data for describing the chemical equilibrium are shown in Table 4 and 5.

In the absence of published values for the decomposition constant for the initiator used in this work, we used values corresponding to the monofunctional initiator cumyl-

Table 3. Kinetic constants for the free radical polymerization of VCM.

Kinetic constants	Units	Refs.
$k_d = 3.7 \times 10^{14} \exp(-13782.8/T_r)$	s^{-1}	[63]
$k_{iA} = k_{iB} = k_p$	$m^3\,kmol^{-1}\,s^{-1}$	This work
$k_p = 5.0 \times 10^7 \exp(-3320/T_r)$	$m^3\,kmol^{-1}\,s^{-1}$	[64]
$k_{tr,m} = k_p 5.78 \exp(-2768/T_r)$	$m^3\,kmol^{-1}\,s^{-1}$	[64]
$k_{t0} = 6.0 \times 10^{-3} \exp(-690.4(1/T_r - 1/T_0))$	$m^3\,kmol^{-1}\,s^{-1}$	This work
$k_{td,1} = 2.0(k_p)^2/k_{t0}$	$m^3\,kmol^{-1}\,s^{-1}$	[64]
$k_{td,2} = k_{td}/((1.7 \times 10 \exp(-1007(1/T_r - 1/T_0))^2)$	$m^3\,kmol^{-1}\,s^{-1}$	This work
$k_{dr} = k_{dp} = 1.0 \times 10 k_d$	s^{-1}	This work
$k_z = 3.2 \times 10^{-1} k_p$	$m^3\,kmol^{-1}\,s^{-1}$	This work

$T_0 = 333.15$ K.

Table 4. Physical parameters used for the diffusion model.

Parameters	Units	Refs.
$T_{g,m} = 70.74$	K	[49]
$T_{g,p} = 87.1 - 0.132(T_r - 273.15) + 273.15$	K	[18]
$\alpha_m = 9.98 \times 10^{-4}$	K^{-1}	[18]
$\alpha_p = 5.47 \times 10^{-4}$	K^{-1}	[18]
$V_{fc} = 0.8(0.025 + \alpha_m(T_r - T_{g,m}))$	–	[18]
$f_{i,o} = 0.60$	–	This work
$\mathbf{A} = \exp(-0.941 \times 10^6 \exp(-4960/T_r))$	–	This work
$\mathbf{B} = \exp(-1.953 \times 10^3 \exp(-2495/T_r))$	–	This work
$\mathbf{C} = \exp(-1.953 \times 10^3 \exp(-2495/T_r))$	–	This work

Table 5. Thermodynamic parameters.

Parameters	Units	Refs.
$P_m^{sat} = \exp(91.43 - 52.7/T_r - 10.98\ln(T_r) + 1.43 \times 10^{-5} T_r^2)$	K, Pa	[65]
$P_w^{sat} = \exp(73.65 - 73.2/T_r - 7.31\ln(T_r) + 4.16 \times 10^{-6} T_r^2)$	K, Pa	[65]
$\sigma_{d,m} = 16$; $\sigma_{p,m} = 6.5$; $\sigma_{h,m} = 2.4$	$(J\,cm^{-3})^{0.5}$	[50]
$\sigma_{d,p} = 18.7$; $\sigma_{p,m} = 9.7$; $\sigma_{h,m} = 7.7$	$(J\,cm^{-3})^{0.5}$	[50]

perneodecanoate (CUPND).[63] According to the work of Zimmerman,[66] the half-life of DIPND at 54 °C is similar to that of CUPND. Given that in the proposed kinetic mechanism, the initiator DIPND is involved in a single decomposition reaction (Equation 1) with a single dissociation constant, the choice seems reasonable. Due to the lack of information, the initiator efficiency was assumed to be similar to values reported for similar reacting systems.[22,63,66] Besides, some of the parameters presented in Table 3 and 4 were adjusted through standard least squares procedures using published[22] and unpublished industrial conversion and average molecular weight data obtained at different reaction temperatures.

In vinyl chloride polymerizations using monofunctional initiators, termination occurs primarily by disproportionation. Green and Paisley[67] examined the MWD of PVC powders using a Schulz[68] distribution and found that the resin has a molar-mass dispersity of 2.0, due to termination by disproportionation and chain transfer to monomer. The same assumption is used here, although detailed information on the performance of bifunctional initiators in suspension VCM polymerizations is not available. In order to consider the possible existence of inhibition steps, typical average impurity composition values present in vinyl chloride were obtained from studies performed by Titova et al.[69] and Zegel'man et al.[70]

3. Simulation Results

3.1. Monomer Conversion and Molecular Weight Averages

Figure 3 compares the experimental data at different temperatures with the model results. In order to test the sensitivity of the model, Figure 3 also shows simulation results at the reaction temperature of 50 °C. It can be observed that the developed model can reproduce the available experimental data fairly well. The largest error is found at 45 °C for conversions greater than 58%, corresponding to the end of the second reaction stage, which is characterized by the total consumption of vinyl chloride in the monomeric phase. Overall, the model can predict very well the end point of the reaction. It is important to observe that the model was sensitive to changes of the operation temperature, resulting in an excellent predictive capability.

Usually, higher temperatures favor the attainment of higher monomer conversions at the end of the batch when either monofunctional[18] or bifunctional[4] initiators are used. However, it is curious to observe in Figure 3 that, although reaction rates increase with temperature, as expected, the final monomer conversion decreases slightly with temperature when DIPND is used as the initiator, due to the unusual combination of activation energies for this analyzed reaction system.

Figure 4 shows the time evolution of $\overline{M}_w$ for different reaction temperatures. It can be observed that the model predicts that $\overline{M}_w$ depends on the reactor temperature, decreasing with the temperature increase, as it is well known. At the beginning of the process $\overline{M}_w$ is higher due to the heating of the reactor, as already reported in the literature.[71] As the reaction temperature stabilizes, the $\overline{M}_w$ values start to increase until the end of the second stage. One must note that the final $\overline{M}_w$ values change less significantly than the $\overline{M}_w$ values observed during the dynamic trajectory, given the larger temperature variations during reaction start-up.

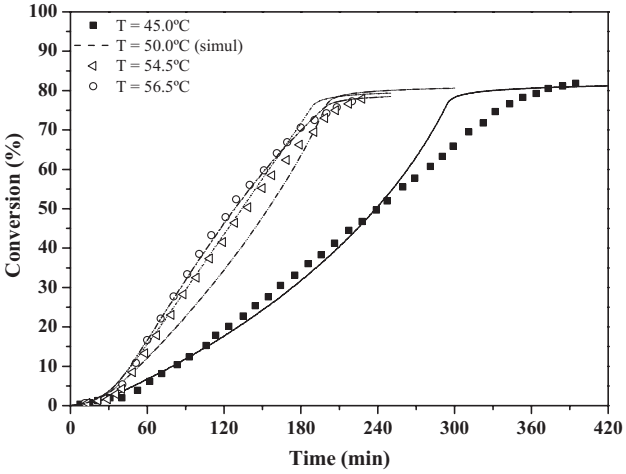

Figure 3. Conversion versus time for $[I] = 0.835$ wt%. Symbols: experimental data;[22] lines: simulations.

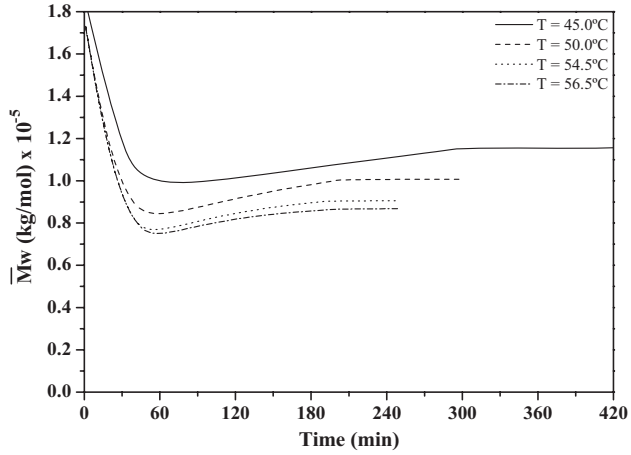

Figure 4. Evolution of weight average molecular weights during reactions for different reaction temperatures ([*I*] = 0.835 wt%).

According to the classical theory on vinyl chloride suspension polymerizations,[16–19,42,71] chain transfer to monomer is strongly influenced by temperature and is independent of the initiator concentration. Thus, the temperature increase is expected to lead to smaller average molecular weights and higher dispersities (due to larger temperature variations), as shown in Figure 5. One might expect that these results reported in the literature for monofunctional initiators should also remain valid for bifunctional initiators, as the reactivity of the active radical species are assumed to be independent of the initiating species.

It must be observed that the ranges of $\overline{M}_w$ values presented in Figure 4 and the polydispersities presented in Figure 5 are very similar to values of typical commercial products produced in the same temperature ranges.[35,36,62]

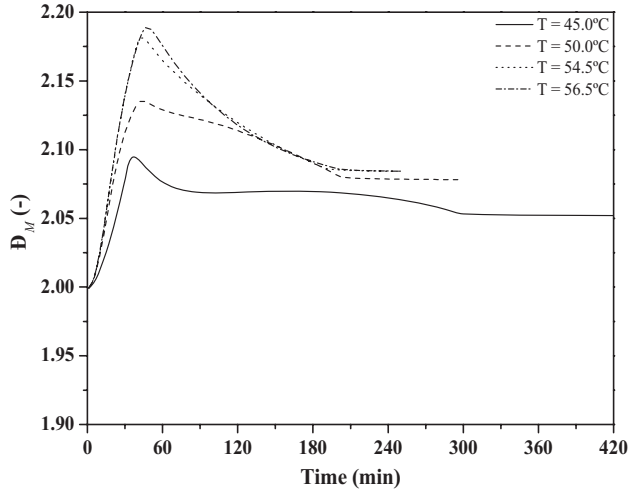

Figure 5. Evolution of the dispersity index at different temperatures at [*I*] = 0.835 wt%.

Therefore, it seems natural to wonder how the use of bifunctional initiators can affect the final properties of the produced resin. First of all, as it is assumed that the decomposition of peroxide groups takes place at random, Figure 6 and 7 show respectively how the average molecular weights and dispersities are expected to change with the fraction of decomposed peroxide groups. In order to build Figure 6 and 7, it was assumed for simplicity that the chain growth probability remains constant throughout the reaction course and that a bifunctional initiator generates two short chains when a single peroxide group is decomposed and generates two short chains and a long

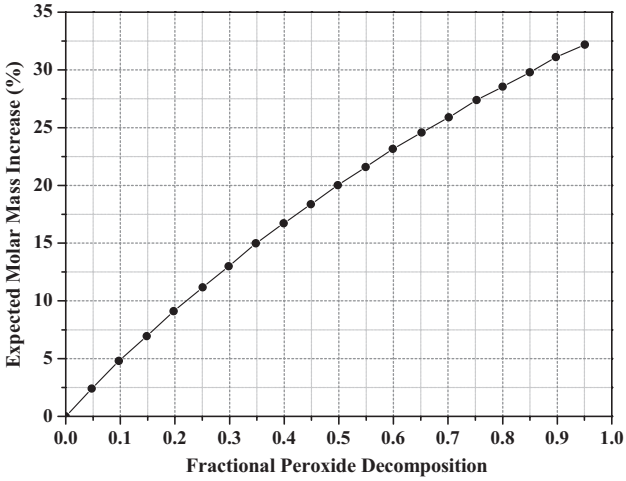

Figure 6. Expected increase of the weight average molecular weight as a function of the fractional initiator decomposition when the growth probability is constant.

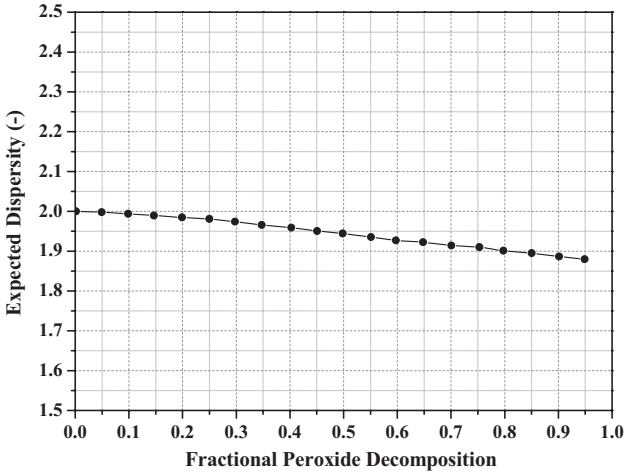

Figure 7. Expected decrease of the dispersity as a function of the fractional initiator decomposition when the growth probability is constant.

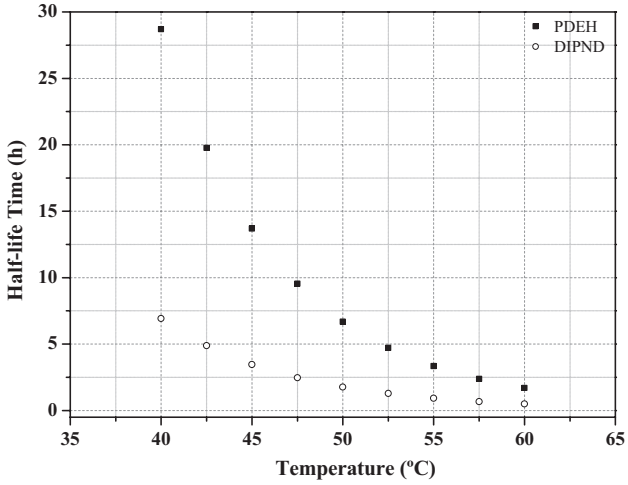

Figure 8. Half-life of PDEH and DIPND at different temperatures.

chain when the two peroxide groups are decomposed simultaneously. Surprisingly, one can see that the use of bifunctional initiators can only exert a significant effect on the molecular weight averages and dispersities of the final polymer chains if very high conversions of peroxide groups can be attained. (For illustrative purposes, Figure 8 shows the half-life values of DIPND at different temperatures, indicating that total decomposition can be expected after 3 h of reaction at temperatures above 40 °C.) This explains why dispersity values are always close to 2 in Figure 5, despite the use of the bifunctional initiator, as observed in standard PVC reactions.

As a matter of fact, Figure 6 and 7 are very optimistic, in the sense that modification of temperatures and compositions during the batch affect the growth probability very strongly and certainly control the evolution of the molecular weight averages and MWDs. Besides, the number of short chains generated by each initiator molecule is certainly larger than 2, due to chain transfer to monomer. As a consequence, one should not expect pronounced modifications of the MWDs of the final PVC resin only because of the presence of multiple peroxide groups in the initiator molecule when this type of bifunctional initiator is used to perform the polymerization reactions, as the experimental data of Krallis et al.[22] also indicate. In this aspect, the availability of a good model can be of fundamental importance for testing of operation procedures and of initiators with alternative molecular structures, including cyclic initiators.

When the performances of the monofunctional initiator di(2-ethylhexyl)peroxydicarbonate (PDEH) and of the bifunctional initiator (DIPND) are compared to each other, as presented by Krallis et al.,[22] it can be concluded that the use of PDEH as a benchmark may not be adequate. According to the half-life data presented in Figure 8, half-lives of PDEH and DIPND present significant differences in the analyzed temperature range of 45–56 °C. As DIPND is more reactive than PDEH, higher polymerization rates can be achieved in reactions conducted with DIPND, as shown in Figure 16 and 19 by Krallis et al.[22] As CUPND and 3-hydroxy-1,1-dimethylbutylperoxyneodecanoate (LUP610) present more similar half-lives when compared to DIPND, as shown in Table 6, comparison of performances seems more appropriate when CUPND (or LUP610) and DIPND are used as the initiating systems.

Conversion profiles for different initiator concentrations are shown in Figure 9. As expected, higher initiator concentrations increase the reaction rates, decreasing the total reaction time, as illustrated in Figure 10. In the particular case of VCM polymerizations performed in suspension, the reaction rates suffer strong deceleration after the end of the second stage, after complete consumption of the monomer phase. This is believed to be due to the development of strong diffusive limitations, which lead to lower initiator efficiencies and lower rates of propagation, which are combined with the decreasing monomer concentrations in the reacting phase.

As also observed experimentally in several systems that use monofunctional initiators,[16,18,73] the critical increase of the reaction rate occurs almost simultaneously with the start of the pressure drop of the system, indicating the complete consumption of the monomer-rich phase. When the polymer concentration is sufficiently high in the reaction medium, the macro-radicals become entangled with other polymeric chain segments, causing the decrease of the diffusion rates and of the frequency of collisions of macro-radicals. The increasing reaction rates that are characteristic of PVC reactions lead to increasing rates of heat production during the batch, requiring investment in

Table 6. Half-life data for peroxide initiators.[63,72]

Peroxide initiator	Temp., °C for half-life times		
	0.1 [h]	1.0 [h]	10 [h]
3-Hydroxy-1,1-dimethylbutylperoxyneodecanoate (LUP610)[63]	91	54	37
1,3-Di(2-neodecanoylperoxyisopropyl)benzene (DIPND)[72]	80	54	35
Cumyl perneodecanoate (CUPND)[63]	76	56	38

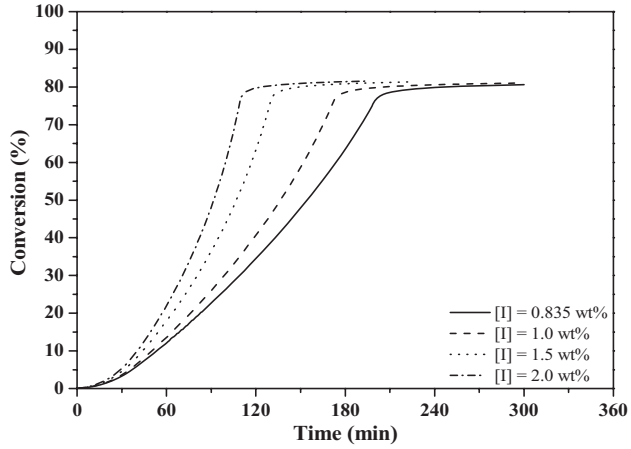

Figure 9. Evolution of conversion at different initiator concentrations ($T_r = 50\ ^\circ C$).

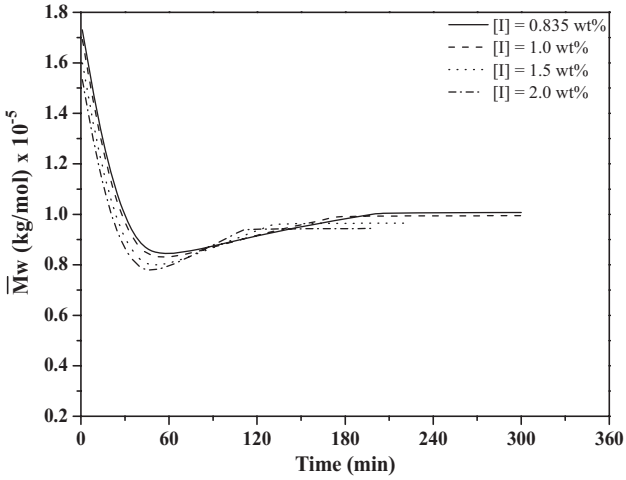

Figure 11. Evolution of $\overline{M}_w$ for different initiator concentrations ($T_r = 50\ ^\circ C$).

hardware and technology to avoid runaway conditions at the plant site.

Figure 11 shows the evolution of $\overline{M}_w$ when using different concentrations of initiator. It can be observed that the molecular weight values are not very sensitive to modification of the initiator concentration, given the high rates of chain transfer to monomer.[16–19,42,71] Despite that, it is possible to note the slow decrease of average molecular weights with the increase of the initiator concentration, as one might already expect.[10,12,74,75] Several authors[36,76] reported that the average molecular weights tend to decrease with monomer conversion at high conversions, while others[21,77] did not observe this trend, reporting constant molecular weight values at the last reaction stages, when monofunctional initiators were used. As one can see in Figure 11, the simulation results obtained in the present study indicate very small variations of $\overline{M}_w$ values in the last stages of the reaction, because of the growth of larger molecules, as shown in Figure 6.

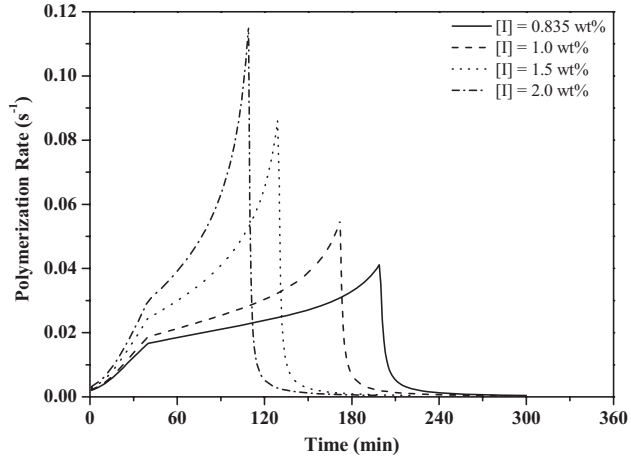

Figure 10. Evolution of the polymerization rate for different concentrations of initiator ($T_r = 50\ ^\circ C$).

3.2. Molecular Weight Distributions

The pgf inversion method employed in the present work for recovering of the MWD from its pgf transform requires the user to specify the value of one parameter, Np, which is the number of terms in the polynomial expansion of the MWD function.[38] Low Np values can produce inaccurate solutions, while high Np values can introduce noise due to error propagation. Thus, the quality of the MWD depends strongly on the selected Np value. In order to evaluate the performance of the proposed numerical method, Asteasuain et al.[38] suggests to compare solutions obtained with different Np values in the form

$$SSQ2_{Np} = \sum_{i=1}^{n_{dp}} \left(x_{Np,DP_i} - x_{Np+1,DP_i}\right)^2 \quad (87)$$

where n_{dp} is the total number of discrete points considered in the MWD, x_{N,DP_i} and x_{N+1,DP_i} are the calculated number or mass fractions for degree of polymerization DP_i, calculated with two successive values of Np. A good value of Np is the one that yields the lowest value of the performance variable SSQ2. Initial guesses for Np should lie between 5 and 12.[38,78] MWD values presented here were always obtained for the optimum Np values.

The pgf technique was applied for degrees of polymerization ranging from 25 to 190 000, using 25 discrete points separated logarithmically for complete recovery of the MWD's. It is evident that both the accuracy of the solution and the computational effort increase with the number of

discretization points used to retrieve the MWD, although tests performed with higher number of discretization points did not lead to any significant improvement of the numerical solutions. The total computational time required to solve each discretized point of the distribution was approximately equal to 9 min. The large computational time was due to the large number of nonlinear differential equations that constitute the model, to the abrupt changes of kinetic constants and model equations during the distinct reaction stages of the batch (especially between the second and the third stages) and to the high numerical accuracy needed for convergence (relative deviation of 1.0×10^{-9}).

Figure 12 shows different calculated MWD's for distinct values of Np at two sampling times (95 and 180 min), when 1.0 wt% of initiator is used at 56.5 °C. The MWD's include are represented as the sums of all kinds of chains (living and dead) that are present in both phases (monomer-rich and polymer-rich). Figure 12 shows that calculated MWD's are similar, although optimum Np values were equal to 10. For this parameter value and using 25 discretization points, approximately 10 500 differential equations are required to perform the reaction simulations. The two sampling times presented in Figure 12 correspond to different reaction stages: (i) at $t = 95$ min, there are four phases in the reaction vessel; (ii) while at $t = 180$ min, the monomer-rich phase is absent. As both situations are very different, Figure 12 illustrates the convergence and robustness of performed model calculations.

Figure 13 and 14 show the MWD evolution during the course of the polymerization when the initiator concentration is equal to 0.875 wt% at temperatures of 50 and 56.5 °C, respectively. The MWD's calculated for conversion of 0.5% are very different from the other ones because the reaction temperatures are still very close to the initial conditions at such low conversions; consequently, the average molecular weights are higher (see Figure 4). As temperature stabilizes, MWD's are first shifted towards lower molecular weight values (due to the higher temperatures) and afterwards shifted slowly toward higher molecular weight values (due to the increasing rates of monomer consumption in the polymer phase and the lower initiator concentrations). As a consequence, the MWD's become broader and the dispersities reach the values of 2.08 at $T = 56.5$ °C and 2.07 at

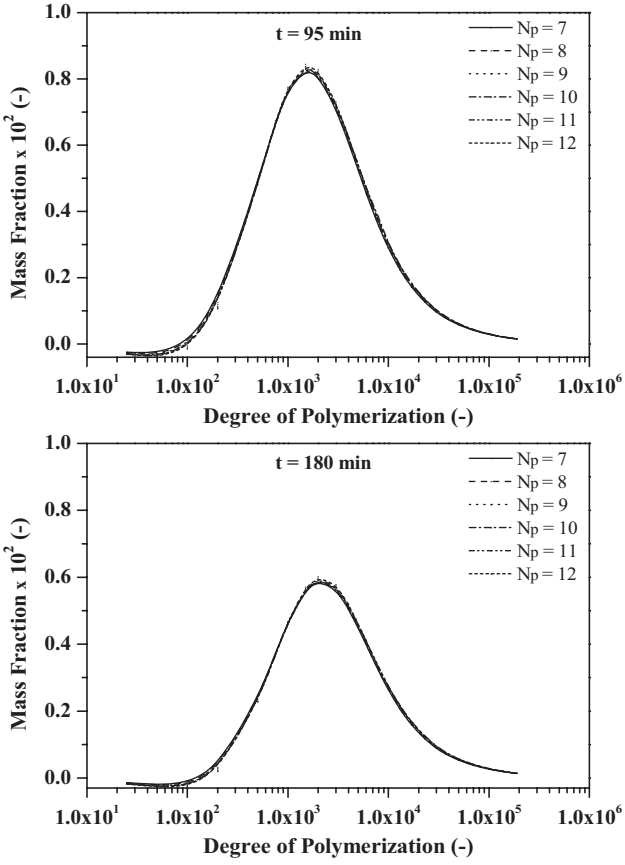

Figure 12. Effect of Np on the predictions of MWD when $[I] = 1$ wt% and $T = 56.5$ °C.

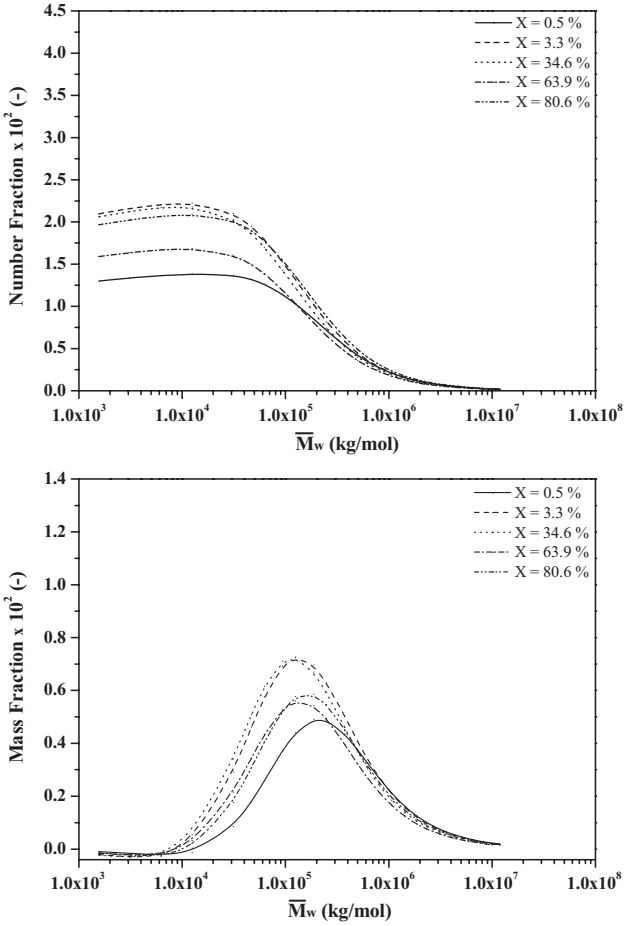

Figure 13. Evolution of (a) molar and (b) mass molecular weight distributions for $[I] = 0.835$ wt% and $T = 50$ °C.

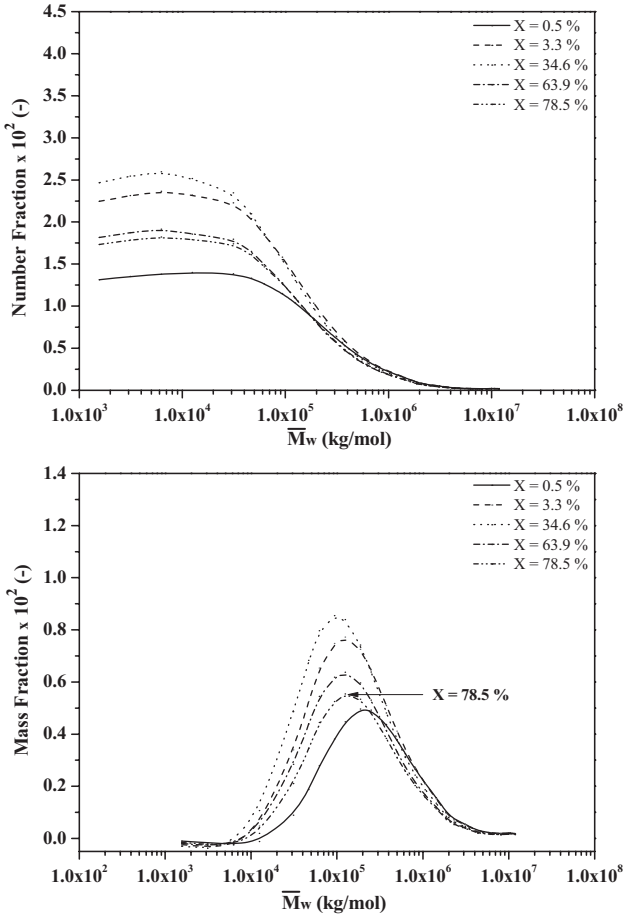

Figure 14. Evolution of (a) molar and (b) mass molecular weight distributions for $[I] = 0.835$ wt% and $T = 56.5$ °C.

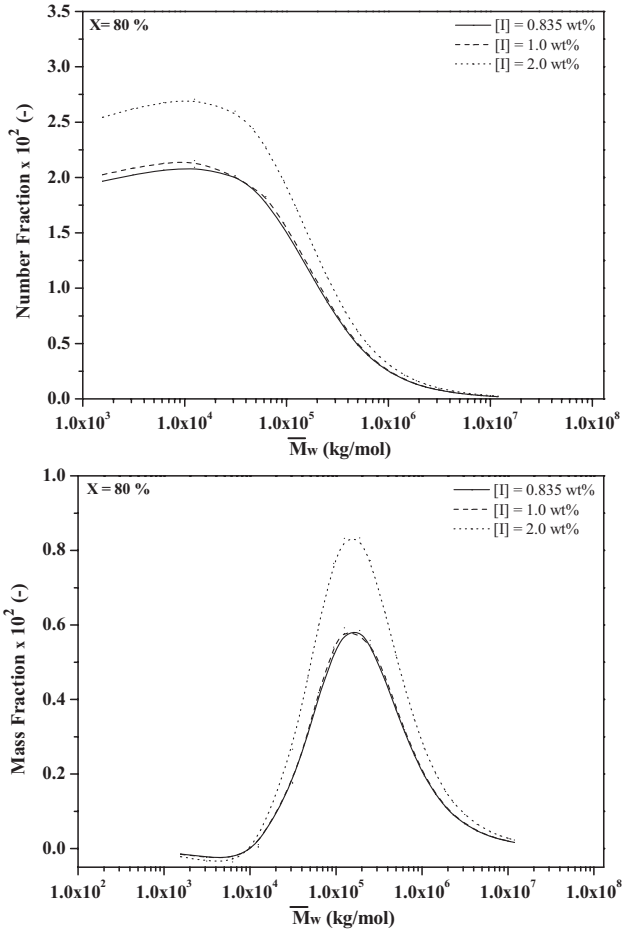

Figure 15. Effect of initiator concentration on the (a) molar and (b) mass molecular weight distributions for $T = 50$ °C.

$T = 50$ °C, which are very close to 2 because of the controlling effect exerted by chain transfer to monomer. Similar results could be obtained in other reaction conditions, including different temperatures and initiator concentrations.

Figure 15 illustrates the effect of initiator concentration on the MWD. All MWDs shown in these figures correspond to the monomer conversion of 80 wt%. One must note that there is no apparent difference in the MWD between the 0.835 and 1.0 wt% of initiator, as one might already expect, given the controlling effect exerted by chain transfer to monomer and the small variation of the initiator concentration. However, by doubling the concentration of initiator, the MWD is shifted toward lower molecular weight values, as one might already expect. Figure 16 shows that sensitivity to the initiator concentration increases with temperature (simulations performed for the reactor temperature of 56.5 °C), due to the higher rates of initiator decomposition and monomer consumption.

As well documented in the literature for commercial PVC resins produced with monofunctional initiators, molar mass distributions are wide, with dispersities slightly above 2.0, as also obtained in all simulations performed in the present study.[79] The MWD of PVC homopolymers approaches a Gaussian distribution (in terms of $\log(\overline{M}_w)$) and does not change much from one manufacturer to another, being independent of the initiator type. The simulations performed here with the bifunctional initiator DIPND confirm these general trends, as already explained and shown in Figure 6 and 7.

It is interesting to observe how the distributions of the distinct polymer species (living, dormant, and dead chains) change during the batch. Figure 17 shows the MWD's of the different polymer chains at different reaction times, for a polymerization run performed at $T = 56.5$ °C and with $[I] = 0.835$ wt%.

It can be observed in Figure 17 that in the early stages of the reaction the concentrations of dead polymer chains P_A in the monomer-rich phase are high. As the reaction

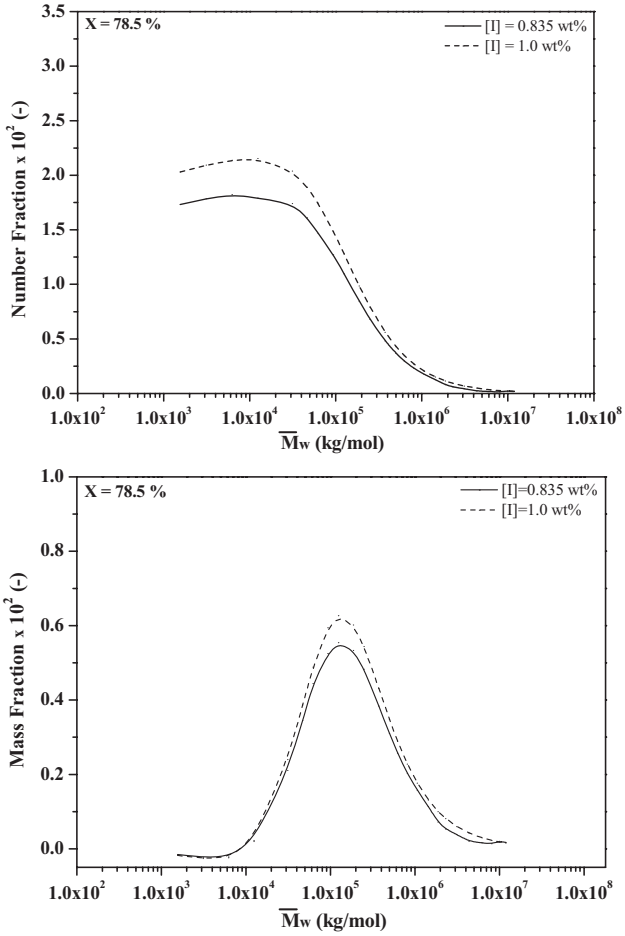

Figure 16. Effect of initiator concentration on the (a) molar and (b) mass molecular weight distributions for $T = 56.5\ ^{\circ}C$.

proceeds, there is a gradual increase in the concentration of chains in the polymer-rich phase, mainly dead chains of type P_A and dormant chains of type P_B. However, as observed previously, due to chain transfer to monomer and the dynamics of the initiator decomposition, the concentrations of chains of type P_B are much smaller than the concentrations of chains of type P_A. The other types of macromolecular chains are always present in very low concentrations and exert little influence on the overall shape of the MWD. The MWD's of P_A and P_B chains are different in the polymer-rich and monomer-rich phases, being shifted toward higher values in the polymer-rich phase because of the gel effect and distinct set of kinetic constants.

4. Conclusions

This study presented a mathematical model for the suspension polymerization of vinyl chloride performed with symmetrical bifunctional initiators. The proposed model is able to describe the evolution of average molecular weights and monomer conversion during the reaction batch, but is also able to simulate the MWDs of macromolecular chains of different types that are present in the monomer-rich and polymer-rich phases. Although the obtained distributions could not be compared with available experimental data, calculated average molecular weights agree well with experimental data available in the literature.

As shown throughout many examples, the dynamics of the MWDs in vinyl chloride suspension polymerizations is controlled by chain transfer to monomer, which makes the MWDs of the final polymer resin little sensitive to the presence of the linear bifunctional initiator. According to the simulations performed here, the MWDs of the final resin are much more sensitive to temperature variations than to variations of the bifunctional initiator concentrations, which is in accordance with a simplified stochastic analysis. One of the reasons that justify the observed small sensitivity is the fact that bifunctional initiator molecules generate more than two short dead chains (growth in one direction) for each long chain (growth in two directions) formed by the decomposition of the two peroxide groups, as shown when the MWDs of all types of macromolecular chains are computed for each reacting phase. Therefore, multifunctional initiators with more complex molecular structure should be considered for PVC reactions, if significant modification of the MWD is pursued.

The model presented here can be used as a tool for tailoring the MWDs of PVC resins obtained through the free radical mechanism using multifunctional initiators. Particularly, the model can be used in the near future to analyze the sensitivity of the final resin properties to modification of the kinetic rate constants and the molecular structure of the multifunctional initiator.

Appendix A

The method developed by Flory and Huggins is useful for estimating the activity coefficient of a solvent of low molecular weight in a polymer solution, whose coefficient is defined as

$$\ln(a_m) = \ln(a_m^{comb}) + \ln(a_m^{res}) \tag{A.1}$$

where the first term on the right side represents a combinatorial contribution corresponding to the entropy of mixing and the second term accounts for the effects of the interaction energy between the lattice sites, also declared as a residual term.

$$\ln(a_m^{comb}) = \ln(1-\phi_p) + \left(1 - \frac{1}{r}\right)\phi_p \tag{A.2}$$

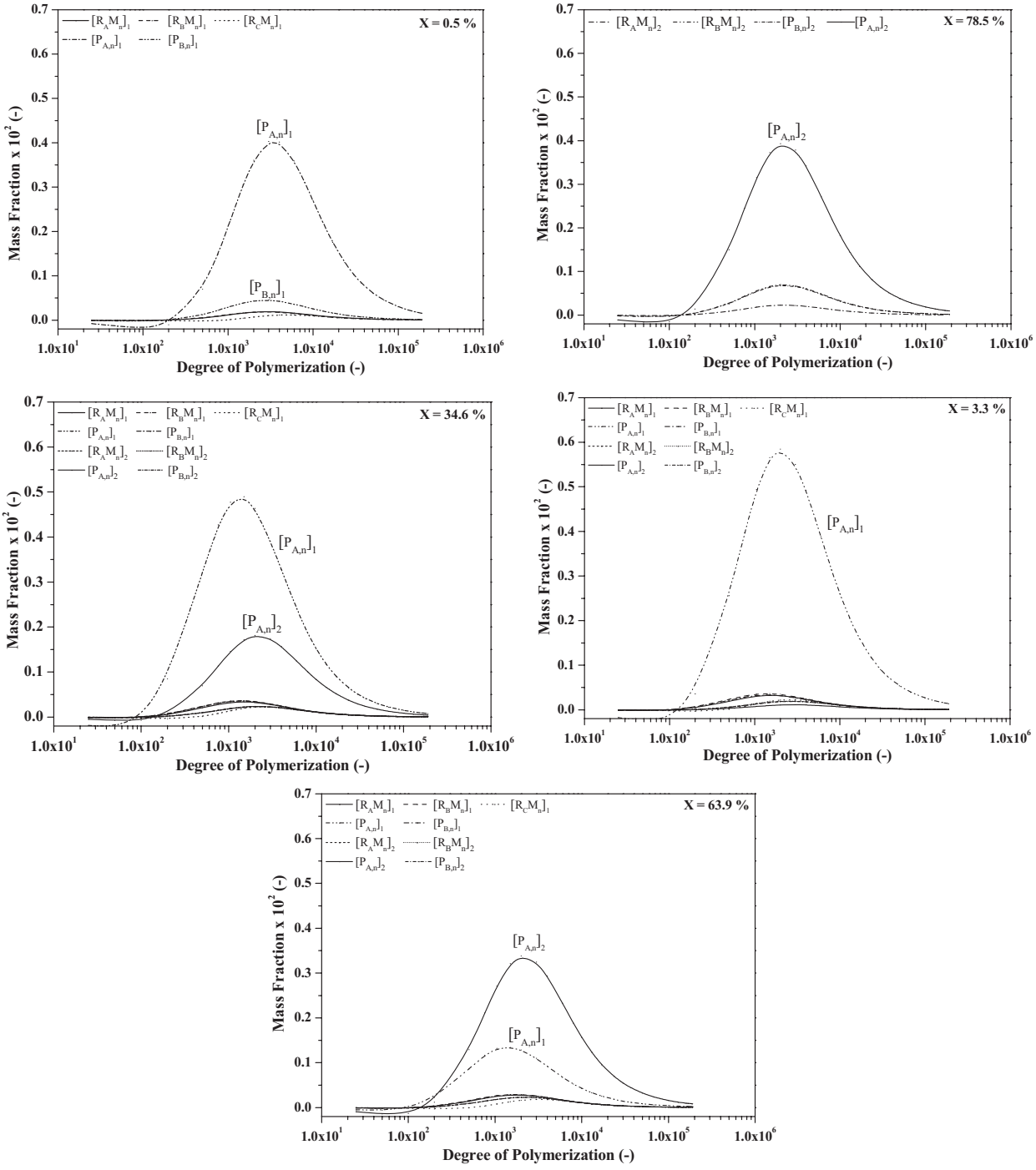

Figure 17. Evolution of the MWD of the different macromolecular species for $[I] = 0.835$ wt% and $T = 56.5\,^{\circ}C$.

$$\ln(a_m^{res}) = \chi_{FH}\phi_p^2 \tag{A.3}$$

$$\ln(a_m) = \ln(1-\phi_p) + \left(1-\frac{1}{r}\right)\phi_p + \chi_{FH}\phi_p^2 \tag{A.4}$$

where ϕ_p is volume fraction of polymer in solution, r is the number of segments in the polymer chain and χ_{FH} is a dimensionless interaction parameter, also known as the Flory Chi parameter.[47] The r factor is related to the size of the chains according to the following equation

$$r = \frac{\vartheta_p MM_p}{\vartheta_m MM_m} \tag{A.5}$$

where ϑ is the specific volume and *MM* is the molecular weight of a component (monomer and polymer) in solution. The segments of chains contained in the polymeric matrix are assumed to occupy the same volume of the solvent molecules. This assumption is quite acceptable for polymer solutions in their own monomer, which is the case here. As the molecular weight of the PVC studied in this work is of the order of 10^4–10^5, is also quite reasonable to consider $1/r \to 0$. Thus:

$$\ln(a_m) = \ln(1-\phi_p) + \phi_p + \chi_{FH}\phi_p^2 \quad (A.6)$$

The polymer–solvent interaction parameter χ_{FH} is considered as a free energy parameter with entropic and enthalpic contributions, defined by

$$\chi_{FH} = \chi_S + \chi_H \quad (A.7)$$

where χ_H is the enthalpic contribution, related to the heat of mixing, while the entropic contribution χ_S is the correction factor, usually defined as a constant and equal to 0.34[48]

$$\chi_H = \frac{\nu_m}{RT_r}(\sigma_m - \sigma_p)^2 \quad (A.8)$$

where υ_{mM} is the molar volume of the solvent (VCM in our case), σ_m and σ_p are the solubility parameters of VCM and PVC, respectively. The molar volume of the VCM was calculated from the Group Contribution Theory.[49] According to Hansen,[48] the total solubility parameter may be calculated from the contributions of three types of interactions,

$$\sigma^2 = \sigma_d^2 + \sigma_{dd}^2 + \sigma_h^2 \quad (A.9)$$

where σ_d^2, σ_{dd}^2, and σ_h^2 are the contributions to the solubility parameter of the dispersive forces, dipole-dipole forces and hydrogen bonding forces, respectively.

Considering that both PVC and water present very low solubility in the monomer-rich phase, it is reasonable to consider that the mole fraction of VCM is approximately equal to 1. Thus,

$$f_{m,2} = P_m^{sat}\exp(\ln(1-\phi_{p,2}) + \phi_{p,2} + \chi_{FH}\phi_{p,2}^2) \quad (A.10)$$

As the partial pressure of the monomer becomes equal to its saturation pressure, one can calculate the volume fraction of polymer in the polymer phase from a non-linear equation (Equation A.11), by using a numerical method

$$0 = \ln(1-\phi_{p,2}) + \phi_{p,2} + \chi_{FH}\phi_{p,2}^2 \quad (A.11)$$

Acknowledgements: The authors thank CNPq (Conselho Nacional de Desenvolvimento Científico e Tecnológico, Brazil), FAPERJ (Fundação Carlos Chagas Filho de Apoio à Pesquisa do Estado do Rio de Janeiro), and Braskem for scholarships, financial and technical support. The authors also thank UNS (Universidad Nacional del Sur, Argentina), CONICET (Consejo Nacional de Investigaciones Científicas y Técnicas, Argentina), and ANPCyT (Agencia Nacional de Promoción Científica y Tecnológica, Argentina) for financial support.

Received: April 21, 2014; Revised: June 1, 2014; Published online: July 17, 2014; DOI: 10.1002/mats.201400038

Keywords: bifunctional initiator; mathematical model; molecular weight distribution (mwd); probability generating function (pgf); suspension polymerization; vinyl chloride

[1] W. P. Yang, C. W. Macosko, S. T. Wellinghoff, *Polymer* **1986**, *27*, 1235.
[2] F. Machado, E. L. Lima, J. C. Pinto, *Polím.: Ciênc. Tecnol.* **2007**, *17*, 166.
[3] R. Dhib, J. Gao, A. Penlidis, *Polym. React. Eng.* **2000**, *8*, 299.
[4] M. Benbachir, D. Benjelloun, *Polymer* **2001**, *42*, 7727.
[5] J. R. Cerna, G. Morales, G. N. Eyler, A. I. Canizo, *J. Appl. Polym. Sci.* **2002**, *83*, 1.
[6] S. Fityani-Trimm, R. Dhib, A. Penlidis, *Macromol. Chem. Phys.* **2003**, *204*, 436.
[7] W.-C. Sheng, J.-Y. Wu, G.-R. Shan, Z.-M. Huang, Z.-X. Weng, *J. Appl. Polym. Sci.* **2004**, *94*, 1035.
[8] M. Asteasuain, A. Brandolin, C. Sarmoria, *Polymer* **2004**, *45*, 321.
[9] W.-C. Sheng, G.-R. Shan, Z.-M. Huang, Z.-X. Weng, Z. Pan, *Polymer* **2005**, *46*, 10553.
[10] M. J. Scorah, R. Dhib, A. Penlidis, *J. Polym. Sci.: Part A: Polym. Chem.* **2004**, *42*, 5647.
[11] G. P. Barreto, G. N. Eyler, *Polym. Bull.* **2011**, *67*, 1.
[12] M. J. Scorah, R. Cosentino, R. Dhib, A. Penlidis, *Polym. Bull.* **2006**, *51*, 157.
[13] L. Soljic, T. Penovic, A. Jukic, Z. Janovic, *AIDIC Conf. Ser.* **2009**, *09*, 283.
[14] V. V. Mazurek, *Vysokomol. Soyed.* **1966**, *7*, 1174.
[15] W. H. Atkinson, C. H. Bamford, G. C. Eastmond, *Trans. Faraday Soc.* **1970**, *66*, 1446.
[16] S. I. Kuchanov, D. N. Bort, *Vysokomol. Soyed.* **1973**, *10*, 2393.
[17] A. K. Suresh, M. Chanda, *Eur. Polym. J.* **1982**, *18*, 607.
[18] T. Y. Xie, A. E. Hamielec, P. E. Wood, D. R. Woods, *Polymer* **1991**, *32*, 537.
[19] C. Kiparissides, G. Daskalakis, D. S. Achilias, E. Sidiropoulou, *Ind. Eng. Chem. Res.* **1997**, *36*, 1253.
[20] J. M. Pinto, R. Giudici, *Chem. Eng. Sci.* **2001**, *56*, 1021.
[21] T. D. Roo, J. Wieme, G. J. Heynderickx, G. B. Marin, *Polymer* **2005**, *46*, 8340.
[22] A. Krallis, C. Kotoulas, S. Papadopoulos, C. Kiparissides, J. Bousquet, C. Bonardi, *Ind. Eng. Chem. Res.* **2004**, *43*, 6382.
[23] W. H. Ray, *J. Macromol. Sci. Part C: Polym. Rev.* **1972**, *C8*, 1.
[24] R. A. Jackson, P. A. Small, K. S. Whiteley, *J. Polym. Sci.: Polym. Chem. Ed.* **1973**, *11*, 1781.
[25] T. Xie, A. E. Hamielec, *Macromol. Theor. Simul.* **1993**, *2*, 455.
[26] P. Pladis, C. Kiparissides, *Chem. Eng. Sci.* **1998**, *53*, 3315.
[27] A. Brandolin, C. Sarmoria, A. Lótpez-Rodríguez, K. S. Whiteley, B. D. A. Fernandez, *Polym. Eng. Sci.* **2001**, *41*, 1413.
[28] H. Tobita, *Macromolecules* **1995**, *28*, 5119.
[29] I. A. Gianoglio Pantano, M. Asteasuain, C. Sarmoria, A. Brandolin, *Macromol. React. Eng.* **2012**, *6*, 406.

[30] A. Krallis, D. Meimaroglou, C. Kiparissides, *Chem. Eng. Sci.* **2008**, *63*, 4342.
[31] C. Kiparissides, P. Seferlis, G. Mourikas, A. J. Morris, *Ind. Eng. Chem. Res.* **2002**, *41*, 6120.
[32] P. D. Iedema, H. C. J. Hoefsloot, *Macromolecules* **2003**, *36*, 3632.
[33] D. Meimaroglou, A. Krallis, V. Saliakas, C. Kiparissides, *Macromolecules* **2007**, *40*, 2224.
[34] J. Lyngaae-Jørgensen, *J. Polym. Sci. Part C: Polym. Symp.* **1971**, *33*, 39.
[35] A. H. Abdel-Alim, A. E. Hamielec, *J. Appl. Polym. Sci.* **1972**, *16*, 783.
[36] T. Y. Xie, A. E. Hamielec, P. E. Wood, D. R. Woods, *Polymer* **1991**, *32*, 1098.
[37] M. Asteasuain, C. Sarmoria, A. Brandolin, *Polymer* **2002**, *43*, 2513.
[38] M. Asteasuain, A. Brandolin, C. Sarmoria, *Polymer* **2002**, *43*, 2529.
[39] W. J. Yoon, *Korean J. Chem. Eng.* **1996**, *13*, 88.
[40] W. H. Starnes, Jr., F. C. Schilling, I. M. Plitz, R. E. Cais, D. J. Freed, R. L. Hartless, F. A. Bovey, *Macromolecules* **1983**, *16*, 790.
[41] W. H. Starnes, Jr., *Proc. Chem.* **2012**, *4*, 1.
[42] A. Crosato-Arnaldi, P. Gasparini, G. Talamini, *Die Makromol. Chem.* **1968**, *117*, 140.
[43] P. T. Delassus, D. D. Schmidt, *J. Chem. Eng. Data* **1981**, *26*, 274.
[44] R. P. Danner, M. S. High, *Handbook of Polymer Solution Thermodynamics*, 1st ed. Wiley-AIChE, New York **1993**.
[45] J. M. Prausnitz, R. N. Lichtenthaler, E. G. Azevedo, *Molecular Thermodynamics of Fluid-Phase Equilibria*. 3rd Prentice Hall PTR, New Jersey – EUA **1998**.
[46] J. C. Huang, R. D. Deanin, *Fluid Phase Equilib.* **2005**, *227*, 125.
[47] P. J. Flory, *Discuss. Faraday Soc.* **1970**, *49*, 7.
[48] C. M. Hansen, *Ind. Eng. Chem. Prod. Res. Dev.* **1969**, *8*, 2.
[49] R. F. Fedors, *Polym. Eng. Sci.* **1974**, *14*, 147.
[50] C. Hansen, *Hansen Solubility Parameters: A User's Handbook*, 2nd ed., Taylor & Francis Group, New York – EUA **2007**.
[51] P. M. Goldfeder, V. A. Volpert, *Math. Probl. Eng.* **1998**, *4*, 377.
[52] G. A. O'Neil, M. B. Wisnudel, J. M. Torkelson, *AIChE J.* **1998**, *44*, 1226.
[53] E. T. Denisov, T. G. Denisova, T. S. Pokidova, *Handbook of Free Radical Initiators*, 1st ed., John Wiley & Sons, Inc., New Jersey – EUA **2003**.
[54] P. J. Flory, *Principles of Polymer Chemistry*. 1st ed. Cornell University Press, New York **1953**.
[55] M. H. Cohen, D. Turnbull, *J. Chem. Phys.* **1959**, *31*, 1164.
[56] M. Asteasuain, M. V. Pérez, C. Sarmoria, A. Brandolin, *Latin Am. Appl. Res.* **2003**, *3*, 241.
[57] M. Asteasuain, C. Sarmoria, A. Brandolin, *J. Appl. Polym. Sci.* **2003**, *88*, 1676.
[58] M. Asteasuain, A. Brandolin, *J. Appl. Polym. Sci.* **2007**, *105*, 2621.
[59] D. R. Miller, C. W. Macosko, *J. Polym. Sci. Part B – Phys.* **1988**, *26*, 1.
[60] I. Visual Numerics, *IMSL Numerical Libraries*. Houston, USA **2010**.
[61] L. F. Albright, Y. Soni, *J. Macromol. Sci. : Part A – Chem.* **1982**, *17*, 1065.
[62] A. R. Tacidelli, J. J. N. Alves, L. G. S. Vasconcelos, R. P. Brito, *Chem. Eng. Process.: Process Intensification* **2009**, *48*, 485.
[63] *Organic Peroxides – Their Safe Handling and Use*, Arkema Canada Inc., Philadelphia – EUA **2006**.
[64] E. Sidiropoulou, C. Kiparissides, *J. Macromol. Sci. : Part A – Chem.* **1990**, *27*, 257.
[65] R. H. Perry, D. W. Green, J. O. Maloney, *Perry's Chemical Engineers' Handbook*, 7th ed., McGraw-Hill, New York – EUA **1997**.
[66] H. Zimmermann, *J. Vinyl Addit. Technol.* **1996**, *2*, 287.
[67] J. H. S. Green, H. M. Paisley, *Research (London)* **1961**, *14*, 170.
[68] G. V. Schulz, *Z. Phys. Chem.* **1935**, *30(B)*, 379.
[69] V. A. Titova, V. I. Zegel'man, A. Y. Pessina, V. A. Popov, D. N. Bort, *Polym. Sci. USSR* **1982**, *24*, 1360.
[70] V. I. Zegel'man, V. A. Titova, V. Y. Kolesnikov, S. I. Miroshnichenko, V. A. Popov, *Polym. Sci. USSR* **1985**, *27*, 882.
[71] J. Wieme, T. D. Roo, G. B. Marin, G. J. Heynderickx, *Ind. Eng. Chem. Res.* **2007**, *46*, 1179.
[72] S. Servaty, W. Geyer, N. Rau, M. Krieg, (Roehm GmbH & CO KG), *United States Patent 6670405*, (**2003**).
[73] T. Mejdell, T. Pettersen, C. Naustdal, H. F. Svendsen, *Chem. Eng. Sci.* **1999**, *54*, 2459.
[74] K. J. Kim, W. Liang, K. Y. Choi, *Ind. Eng. Chem. Res.* **1989**, *28*, 131.
[75] L. Cavin, A. Rouge, T. Meyer, A. Renken, *Polymer* **2000**, *41*, 3925.
[76] E. M. Sörvik, *J. Polym. Sci.: Polym. Lett. Ed.* **1976**, *14*, 735.
[77] A. F. Cebollada, M. J. Schmidt, J. N. Farber, N. J. Capiati, E. M. Vallés, *J. Appl. Polym. Sci.* **1989**, *37*, 145.
[78] C. Sarmoria, M. Asteasuain, A. Brandolin, *Can. J. Chem. Eng.* **2012**, *90*, 263.
[79] G. Pepperl, *J. Vinyl Addit. Technol.* **2000**, *6*, 88.